The Journal of Experimental Biology 212, 1949-1964
Published by The Company of Biologists 2009
doi:10.1242/jeb.028464

Regulation of gill transcellular permeability and renal function during acute hypoxia in the Amazonian oscar (*Astronotus ocellatus*): new angles to the osmorespiratory compromise

Chris M. Wood[1,2,*], Fathima I. Iftikar[1], Graham R. Scott[3], Gudrun De Boeck[4], Katherine A. Sloman[5], Victoria Matey[6], Fabiola X. Valdez Domingos[7], Rafael Mendonça Duarte[7], Vera M. F. Almeida-Val[7] and Adalberto L. Val[7]

[1]Department of Biology, McMaster University, Hamilton, Ontario, Canada, L8S 4K1, [2]Division of Marine Biology and Fisheries, Rosenstiel School of Marine and Atmospheric Science, University of Miami, Miami, FL 33149, USA, [3]Department of Zoology, University of British Columbia, Vancouver, Canada, V6T 1Z4, [4]Department of Biology, University of Antwerp, Groenenborgerlaan 171, B-2020 Antwerp, Belgium, [5]School of Biological Sciences, University of Plymouth, Devon PL4 8AA, UK, [6]Department of Biology, San Diego State University, 5500 Campanile Drive, San Diego, CA 92182, USA and [7]Laboratory of Ecophysiology and Molecular Evolution, Instituto Nacional de Pesquisas da Amazônia (INPA), Manaus, Brazil

*Author for correspondence (e-mail: woodcm@mcmaster.ca)

Accepted 16 March 2009

SUMMARY

Earlier studies demonstrated that oscars, endemic to ion-poor Amazonian waters, are extremely hypoxia tolerant, and exhibit a marked reduction in active unidirectional Na^+ uptake rate (measured directly) but unchanged net Na^+ balance during acute exposure to low P_{O_2}, indicating a comparable reduction in whole body Na^+ efflux rate. However, branchial O_2 transfer factor does not fall. The present study focused on the nature of the efflux reduction in the face of maintained gill O_2 permeability. Direct measurements of ^{22}Na appearance in the water from bladder-catheterized fish confirmed a rapid 55% fall in unidirectional Na^+ efflux rate across the gills upon acute exposure to hypoxia (P_{O_2}=10–20 torr; 1 torr=133.3 Pa), which was quickly reversed upon return to normoxia. An exchange diffusion mechanism for Na^+ is not present, so the reduction in efflux was not directly linked to the reduction in Na^+ influx. A quickly developing bradycardia occurred during hypoxia. Transepithelial potential, which was sensitive to water [Ca^{2+}], became markedly less negative during hypoxia and was restored upon return to normoxia. Ammonia excretion, net K^+ loss rates, and ^3H_2O exchange rates (diffusive water efflux rates) across the gills fell by 55–75% during hypoxia, with recovery during normoxia. Osmotic permeability to water also declined, but the fall (30%) was less than that in diffusive water permeability (70%). In total, these observations indicate a reduction in gill transcellular permeability during hypoxia, a conclusion supported by unchanged branchial efflux rates of the paracellular marker [^{3}H]PEG-4000 during hypoxia and normoxic recovery. At the kidney, glomerular filtration rate, urine flow rate, and tubular Na^+ reabsorption rate fell in parallel by 70% during hypoxia, facilitating additional reductions in costs and in urinary Na^+, K^+ and ammonia excretion rates. Scanning electron microscopy of the gill epithelium revealed no remodelling at a macro-level, but pronounced changes in surface morphology. Under normoxia, mitochondria-rich cells were exposed only through small apical crypts, and these decreased in number by 47% and in individual area by 65% during 3 h hypoxia. We suggest that a rapid closure of transcellular channels, perhaps effected by pavement cell coverage of the crypts, allows conservation of ions and reduction of ionoregulatory costs without compromise of O_2 exchange capacity during acute hypoxia, a response very different from the traditional osmorespiratory compromise.

Key words: sodium flux, potassium flux, PEG-4000, diffusive water flux, urine flow rate, glomerular filtration rate, gill morphology, mitochondria rich cell, transepithelial potential, fish.

INTRODUCTION

The traditional osmorespiratory compromise in freshwater fish refers to the trade-off that occurs between increased respiratory gas exchange and osmoregulatory deficit at the gills (Randall et al., 1972; Nilsson, 2007). A highly permeable gill with a large surface area is required for efficient gas transfer; however a small, impermeable epithelium is required to minimize diffusive ion losses and water gain. The phenomenon is well-documented during exercise in fish, with increased Na^+ losses and water gain occurring early on during swimming activity, followed by partial or complete correction later on as compensatory mechanisms are activated (Wood and Randall, 1973a; Wood and Randall, 1973b; Gonzalez and McDonald, 1992; Gonzalez and McDonald, 1994; Postlethwaite and McDonald, 1995). Environmental hypoxia is another situation where demands for respiratory gas exchange are increased. The concept of the osmorespiratory compromise has recently been examined in the context of respiratory deficit caused by ionoregulatory challenge (Greco et al., 1995; Greco et al., 1996; Henriksson et al., 2008), but has received only limited experimental attention in the context of osmoregulatory tradeoffs (e.g. Matey et al., 2008). However, our recent study on the Amazonian oscar *Astronotus ocellatus* reported that unidirectional influx and efflux rates of Na^+ decreased markedly during acute, severe hypoxia (P_{O_2} <20 torr; 1 torr=133.3 Pa) such that net Na^+ balance remained unchanged (Wood et al., 2007). The reduction in whole body Na^+ efflux at a time of hypoxic challenge was surprising. Notably, ammonia and urea loss rates also decreased, and the effects persisted for a short time during normoxic recovery, suggesting that there was a general, regulated reduction in gill

permeability. This is reminiscent of the 'channel arrest' hypothesis proposed to explain survival of the brain and liver in severely hypoxia-tolerant organisms such as turtles and Crucian carp (Hochachka, 1986; Boutilier, 2001; Boutilier and St-Pierre, 2000; Hochacka and Lutz, 2001). This concept envisages that O_2 lack initiates a generalized suppression of ion channel densities and/or channel leak activities, so as to lower the permeability of cell membranes and therefore the energetic costs of maintaining electrochemical gradients. The net consequence is ATP conservation.

Oscars commonly encounter hypoxia in their natural environment when they enter the seasonally flooded jungle to feed and reproduce; adults are reported to survive up to 6 h of complete anoxia, and can tolerate levels of 5–20% air saturation for 20–50 h (Almeida-Val and Hochachka, 1995; Muusze et al., 1998; Almeida-Val et al., 2000). This ability appears to be the result of exceptional capacities to both downregulate aerobic metabolic rate and to survive on glycolytic metabolism (Muusze et al., 1998; Almeida-Val et al., 2000; Sloman et al., 2006; Richards et al., 2007). Thus one possible explanation is that under severe O_2 limitation, oscars do not attempt to increase gill O_2 transfer in a situation where the potential for O_2 uptake from the water has become very slight. Instead they may simply close down the gills to reduce osmoregulatory costs at a time when active ion influx has been reduced by O_2 starvation of the gill ion pumps. To address this possibility, we recently measured ventilation and the branchial O_2 transfer factor in adult oscars exposed to progressive, severe hypoxia, as well as the O_2 consumption rate of isolated gill epithelial cells (Scott et al., 2008). The transfer factor is a measure of the relative ability of the respiratory surface to exchange O_2 and defined as the rate of O_2 consumption divided by the mean P_{O_2} driving force for diffusion across that surface (Randall et al., 1967). Contrary to these interpretations, ventilation increased down to a P_{O_2} of 10 torr, branchial O_2 transfer factor increased down to a P_{O_2} of 20 torr and returned to normoxic levels at 10 torr, and gill epithelial O_2 consumption actually increased down to a P_{O_2} below 5 torr. Thus, oscars increase ventilation and the effective permeability of the gills to O_2 during severe hypoxia in a comparable manner to hypoxia-intolerant teleosts such as trout (Holeton and Randall, 1967; Randall et al., 1967), and there is no evidence that the gill cells are O_2-starved at this time.

Therefore, in the present investigation, which used a normoxia–hypoxia–normoxic recovery regime, our particular focus was to elucidate the mechanism(s) behind the decrease in iono/osmotic permeability which occurs in the absence of a reduction in O_2 permeability during acute hypoxia. Our first objective was to ensure that the previously observed reduction in Na^+ efflux during acute hypoxia was not an artefact of the indirect measurement technique used by Wood et al. (Wood et al., 2007) where efflux was measured in the standard manner (cf. Kirschner, 1970; Wood, 1992) as the difference between radioisotopically determined influx and non-radioactive net flux. Therefore, in the present study, the fish were loaded with ^{22}Na for direct measurement of Na^+ efflux. A further objective was to ensure that the reduction in efflux was a gill phenomenon, by collecting urinary output separately. Another goal was to eliminate the possibility that the Na^+ efflux reduction was simply a consequence of the reduction in Na^+ influx because of possible linkage of the two by exchange diffusion [direct 1:1 coupling of a portion of Na^+ efflux to Na^+ influx (cf. Gonzalez et al., 2002)]. Heart rate and ventilation rate were also measured during the exposure regime to assess how these might contribute to the observed responses. After clarification of these issues, a central objective became the examination of other markers of gill permeability, which might be diagnostic of changes in either paracellular permeability, transcellular permeability, or both during acute hypoxia. These included net K^+ flux, ammonia flux, osmotic water flux (by urine flow rate and weight changes), diffusive water flux (by ^3H_2O exchange), transepithelial potential (TEP), and tritium-labelled polyethylene glycol ([^{3}H]PEG-4000) flux. The latter is a high molecular mass paracellular permeability marker (Wood and Pärt, 1997), which is also an excellent extracellular space (Munger et al., 1991) and glomerular filtration rate marker (Beyenbach and Kirschner, 1976) in teleosts, so this allowed a more detailed assessment of kidney function during acute hypoxia. Finally, we employed scanning electron microscopy to look for morphological correlates of the reduction in gill permeability that was observed. Overall, the results support the hypothesis that reduced iono/osmotic permeability in the gills during severe hypoxia is through channel arrest, i.e. through reduced transcellular permeability.

MATERIALS AND METHODS

Experimental animals

Adult oscars (*Astronotus ocellatus*; Cuvier 1829) were obtained from Sítio dos Rodrigues (Km 35, Rod. AM-010, Brazil), and held for approximately one month prior to experiments at the Ecophysiology and Molecular Evolution Laboratory of the Instituto Nacional de Pesquisas da Amazônia (INPA), in Manaus, Brazil. Fish mass ranged from 67–226 g. Fish were held with natural photoperiod in 500 l tanks, where they were fed a daily 1% ration of commercial pellets (Nutripeixe Tr 36, Purina, São Paulo, SP, Brazil; composition available from the manufacturer). Our analysis yielded the following major electrolyte concentrations in the food: Na^+ 657, Cl^- 457, K^+ 333, Ca^{2+} 418, Mg^{2+} 150 mmol kg^{-1}. The holding and experimental water was typical Amazonian soft water taken from a well on the INPA campus (concentrations in μmol l^{-1}: Na^+ 35, Cl^- 36, K^+ 16, Ca^{2+} 18, Mg^{2+} 4; dissolved organic carbon, 0.6 mg l^{-1} C l^{-1}; pH 6.5) with partial recirculation and continuous filtration, at 28±3°C. Based on findings that gill permeability changes during acute hypoxia were more distinct in starved oscars (G.D.B., unpublished results), fish were fasted for at least 5 days prior to experiments. All experimental procedures complied with Brazilian and INPA animal care regulations.

Experimental protocols

Soft water from the same well-water source as used during holding was employed in all trials. Experimental temperature was 28±1.5°C. Experimental chambers were 2.5 l Nalgene kitchen containers, which fitted the horizontally flattened morphology of the fish. The lids accommodated a portable O_2 probe. The chambers (up to 12 at one time) were mounted on a trough, which served as a water-bath, keeping the external water level slightly below the internal water level for temperature control. The entire trough drained into a vigorously aerated 800 l reservoir, from which water was pumped back to the individual chambers at about 200 ml min^{-1}. Water in the reservoir was replaced daily. Thus each chamber was fitted with an individual water line for flushing, and with an individual air-stone for air or N_2-gassing. Fish were placed in these individual containers the evening before an experiment and left overnight to settle with continuous water flow-through and aeration; black plastic shielding minimized visual disturbance.

The standard protocol, with some variations, was a 3-h control period of normoxia, followed by 3–4 h of acute hypoxia, and then 2–3 h of normoxia again. In order to measure flux rates of various substances, the water inflow into each box was stopped at the

beginning of the experiment, and the level set to a nominal volume of 1.5 l (or kept at 5.5 l in the blood gas trials). Exact volumes were determined by subtracting the mass of the fish when they were weighed at the end of the experiment. Flux rates were generally measured by withdrawing 10 ml or 20 ml water samples for assay at 0.5-h or 1-h intervals, depending on the experiment.

Normoxia (P_{O_2} >130 torr) was maintained by vigorous aeration during the normoxic periods, and water P_{O_2} was checked once per hour in each chamber with the portable O_2 probe. Acute hypoxia was induced by changing the vigorous gassing to N_2, and then maintaining the P_{O_2} between 10–20 torr with more gentle gassing with N_2 or air as required. During the hypoxia period, water P_{O_2} was checked in each chamber every 15 min to ensure it stayed within the target range.

Series 1

The objective of this series was to confirm, by direct measurement, that unidirectional Na^+ efflux (J_{out}^{Na}) fell during acute hypoxia, as previously recorded by indirect measurement (Wood et al., 2007), and that the phenomenon occurred at the gills. This was accomplished by radiolabelling the internal Na^+ pool with ^{22}Na, and recording the appearance of radioactivity in the external water. Na^+ net flux (J_{net}^{Na}) was also recorded, so this approach allowed indirect measurement of Na^+ influx (J_{in}^{Na}, see Calculations section below). Net branchial K^+ and ammonia fluxes were also measured. The oscars were fitted with urinary bladder catheters to collect urine flow outside the chamber, thereby allowing quantification of any renal contribution to the responses. In addition this approach allowed direct measurement of urine flow rate (UFR), an index of osmotic water permeability (e.g. Potts et al., 1967).

Oscars (N=7) were anaesthetized in 0.5 g l^{-1} MS-222 neutralized with 1.0 g l^{-1} $NaHCO_3$ and fitted with internal urinary bladder catheters (Clay-Adams PE50 tubing, with 2 cm PE160 sleeves attached by cyanoacrylate glue) as described by Wood and Patrick (Wood and Patrick, 1994). The sleeves were glued to the catheters and in turn were anchored to the body wall by silk sutures. At this time, each fish received an intra-peritoneal injection of 0.2 ml Cortland saline (Wolf, 1963) containing 10 μCi ^{22}Na (manufactured by New England Nuclear-Dupont, Boston, MA, USA, and supplied by REM, Sao Paulo, Brazil). The oscars were then returned to their individual chambers and allowed to recover overnight (~12 h) while UFR was collected to verify that the catheter was patent. ^{22}Na equilibrates very rapidly in fish; for example, in the killifish, Wood and Laurent (Wood and Laurent, 2003) found no differences in internal radiolabelled Na^+ pool if fish were injected and sampled after only 3 h or allowed to equilibrate for 24 h. Therefore, in the oscar, ^{22}Na was fully equilibrated by the time experiments began the next morning.

Before the start of the experiment, the water in the reservoir was replaced and the fish boxes flushed to remove radioactivity, which had accumulated during the recovery and equilibration period. The chambers were then closed, and fluxes measured by sampling at 1-h intervals during 3 h of normoxia, 4 h of hypoxia, and 2 h of normoxic recovery. Water was analysed for ^{22}Na radioactivity, and the concentrations of total Na^+, K^+ and ammonia. Urine was collected at hourly intervals for analysis of UFR, Na^+, K^+ and ammonia concentrations. At the end of the experiment, the fish were individually anaesthetized as before, and a 0.3 ml blood sample withdrawn by caudal puncture into a heparinized syringe. Plasma was separated by rapid centrifugation (2 min at 7000 ***g***) and analysed for ^{22}Na radioactivity and total Na^+ concentration. The fish were then returned to their chambers under flow-through conditions for overnight recovery before the experiments of Series 3. UFR collection was resumed to ensure continued patency of the urinary catheters.

Series 2

The objective of this series was to employ direct measurements of J_{in}^{Na} to confirm that the patterns previously reported by Wood et al. (Wood et al., 2007) in uncannulated oscars occurred similarly in fish that had previously experienced MS-222 anaesthesia and surgery so as to fit them with urinary bladder catheters. A second objective was to confirm the indirect measurements of J_{in}^{Na} of Series 1. This series also supplied additional data on UFR and urine composition.

Oscars (N=10) were fitted with internal urinary bladder catheters as in series 1, but were not injected with ^{22}Na. After overnight recovery, water flow to the fish chambers was stopped, and 2 μCi of ^{22}Na was added to each chamber and allowed to mix for 1 h. The experiment was then started with the same protocol as in series 1: 3 h of normoxia, 4 h of hypoxia and 2 h of normoxic recovery. Water was sampled hourly for measurement of ^{22}Na radioactivity and total Na^+ concentration, and urine was collected at 1-h intervals for analysis of UFR, Na^+, K^+ and ammonia concentrations. Water samples were also analysed for K^+ in six of the fish. Blood was not sampled at the end of the protocol, but instead oscars were left undisturbed under normoxia (with flow-through water) for an overnight collection of urine to further assess the recovery of UFR.

Series 3

The goal here was to check whether the phenomenon of exchange diffusion (direct 1:1 linkage of a portion of J_{out}^{Na} to J_{in}^{Na}) was present in the gills of oscars. This process was found in approximately half of the Amazonian teleosts surveyed by Gonzalez et al. (Gonzalez et al., 2002), but *Astronotus ocellatus* was not included in that survey.

After overnight recovery, replacement of the water in the reservoir and flushing of the chambers, the urinary-catheterized fish (N=7) originally used in Series 1 were subjected to two successive 3-h flux measurements under normoxia. These oscars were still radiolabelled with the ^{22}Na injected earlier. In the first flux determination, the background Na^+ concentration of the external water ($[Na^+]_{ext}$) was used. In the second, $[Na^+]_{ext}$ was acutely raised approximately 10-fold by addition of sufficient NaCl, so as to stimulate J_{in}^{Na} to approximate maximum transport velocity, according to the J_{in}^{Na} *versus* $[Na^+]_{ext}$ kinetic relationship reported by Wood et al. (Wood et al., 2007). Water ^{22}Na radioactivity and total Na^+ concentrations were measured. At the end of the second flux determination, fish were anaesthetized and blood-sampled as above for assay of plasma ^{22}Na radioactivity and total Na^+ concentration. These determinations allowed direct measurements of J_{out}^{Na} and J_{net}^{Na}, and therefore indirect measurement of J_{in}^{Na}.

Series 4

The goal here was to measure changes in heart rate and breathing rate during the regime. Oscars (N=5) were anaesthetized as above, and fish-hook impedance electrodes (varnish-coated copper wire, bare at the ends) were implanted anterior and posterior to the heart using #22 hypodermic needles. An impedance converter was used to check the positioning. Once a strong signal was achieved, the needles were removed and electrodes were sewn in place to the body wall with silk sutures, and the wires threaded through PE60 tubing to avoid tangling. After overnight recovery, the fish were subjected to a regime of 3 h of normoxia, 3 h of hypoxia, and 3 h of normoxic recovery. Heart rate was recorded using the impedance

converter, and breathing rate was determined visually. Measurements were made at 0, 60, 120 and 180 min of normoxia, at 5, 10, 15, 30, 45, 60, 90, 120, 150 and 180 min of hypoxia, and at 5, 15, 30, 45, 60, 90, 120, 150 and 180 min of normoxic recovery.

Series 5

The objective of this series was to monitor transepithelial potential (TEP) as a potential index of paracellular permeability changes. The intra-peritoneal catheter technique pioneered by Potts and Eddy (Potts and Eddy, 1973), which was validated against blood catheter measurements by Wood and Grosell (Wood and Grosell, 2008), was employed. Oscars (N=7) were anaesthetized as above, and fitted with saline-filled PE50 catheters inserted approximately 3–4 cm into the coelom through a puncture site (made with a no. 19 hypodermic needle) in the lateral body wall. A 2 cm PE160 sleeve, heat-flared at both ends, was glued to the PE50 with cyanoacrylate glue and anchored to the body wall with several silk sutures; this prevented the catheter from changing depth in the coelom.

After overnight recovery, the fish were exposed to 3 h of normoxia, 3 h of hypoxia, and 2 h of normoxic recovery, with hourly measurements of TEP. The fish were then left under normoxic flow-through conditions for a further overnight period. Thereafter, the oscars (now six, because of one catheter failure) were exposed to sequentially increasing concentrations of external Ca^{2+} ($[Ca^{2+}]_{ext}$) under normoxia in half-logarithmic steps. The goal here was to test whether TEP in oscars responded to $[Ca^{2+}]_{ext}$ in the standard manner described for many other teleosts, which is thought to reflect paracellular permeability changes (Potts, 1984). This was achieved by addition of small volumes of a $CaSO_4$ stock solution at 0.5-h intervals. TEP was measured at the end of each 0.5-h period, at nominal $[Ca^{2+}]_{ext}$ concentrations of background (~18 μmol l^{-1}) followed by 100, 320, 1000 and 3200 μmol l^{-1}.

Series 6

Diffusive exchange of water was measured by monitoring the efflux of tritiated water (^3H_2O; manufactured by Perkin-Elmer Wellesley, MA, USA, and supplied by REM, Sao Paulo, Brazil). Intraperitoneal catheters were implanted as in Series 5, and the fish allowed to recover from anaesthesia overnight. In preliminary trials under normoxia, we found that a minimum equilibration period of 1 h was needed after intraperitoneal injection before ^3H_2O efflux rates became stable. Thereafter stable rates could be recorded for 3 h, after which recycling of the radioisotope became a problem, because external specific activity exceeded 10% of internal specific activity (Kirschner, 1970). Therefore it was necessary to use three experimental groups to cover the entire normoxia-hypoxia-normoxic recovery regime.

In the first group, covering the normoxic period, oscars (N=9) were injected under normoxia with ^3H_2O (10 μCi ^3H_2O in 200 μl Cortland saline, washed in with a further 200 μl saline). Injection *via* the intraperitoneal catheter avoided any handling or disturbance of the fish. After 1 h equilibration, water samples were withdrawn at 0.5-h intervals for a further 3 h. In the second group, covering the hypoxic period, oscars (N=10) were injected with the same dose of ^3H_2O under normoxia. However, after 1 h equilibration, hypoxia was instituted, and water samples taken at 0.5-h intervals for a further 3 h under hypoxia. In the third group, covering the normoxic recovery period, the fish (N=8) were first exposed to normoxia, and then to hypoxia for 2 h, at which time they were injected with the same dose of ^3H_2O. After a further 1 h equilibration under hypoxia, normoxia was restored and water samples were taken at 0.5 h intervals for the 3-h period of normoxic recovery. In all three groups, the boxes were then left closed with aeration for approximately 30 h after the original injection. A final water sample was taken to ascertain the exact dose of ^3H_2O which had been administered to each fish, because by this time the radioisotope had completely equilibrated between the fish and the water (see Calculations).

Series 7

The primary objective of this series was to measure the efflux of tritium-labelled polyethylene glycol ([^{3}H]PEG-4000; MW=4000, 1.28 mCi g^{-1}; manufactured by New England Nuclear-Dupont, Boston, MA, and supplied by REM, Sao Paulo, SP, Brazil) as a marker of gill paracellular permeability (Wood and Part, 1997). However since only a small portion of injected [^{3}H]PEG-4000 is excreted *via* the gills in teleosts, and a much larger portion by the kidney (Curtis and Wood, 1991; Scott et al., 2004), it was essential that the fish be fitted with urinary catheters to collect all renally excreted [^{3}H]PEG-4000 outside the fish chambers. Therefore, only branchially excreted [^{3}H]PEG-4000 appeared in the external water. Additionally, this approach allowed us to follow up the results of Series 1 with a more detailed assessment of kidney function, because [^{3}H]PEG-4000 is an excellent glomerular filtration rate marker in teleosts (Beyenbach and Kirschner, 1976).

Oscars (N=12) were fitted with internal urinary bladder catheters as in Series 1. While still anaesthetized, each fish was injected *via* the caudal vein with 8 μCi [^{3}H]PEG-4000 in 0.25 ml of saline, washed in with a further 0.25 ml of saline. The fish were then allowed to recover overnight for approximately 14 h for full equilibration of the label throughout the extracellular compartment (Munger et al., 1991), during which time UFR was monitored to ensure patency of the urinary catheters. Prior to the start of the experiment, the water in the reservoir was replaced and the fish boxes flushed to remove radioactivity that had accumulated during the recovery and equilibration period. The chambers were then closed. The exposure regime consisted of 3 h of normoxia, 3 h of hypoxia, and 3 h of normoxic recovery, with water and urine samples collected at hourly intervals. At the end of the experiment, the fish were individually anaesthetized as before, a 0.3 ml blood ample withdrawn by caudal puncture into a heparinized syringe, and plasma was immediately separated by centrifugation. Water samples were analysed for [^{3}H]PEG-4000 radioactivity, and plasma and urine samples were assayed for [^{3}H]PEG-4000 radioactivity and Na^+ concentration. These measurements allowed calculation of gill [^{3}H]PEG-4000 clearance rate, glomerular filtration rate (GFR, equivalent to renal [^{3}H]PEG-4000 clearance rate), and renal Na^+ handling (see Calculations below).

Series 8

Reductions in UFR recorded in Series 1, 2 and 7 suggested that osmotic water permeability (cf. Potts et al., 1967) was reduced during hypoxia. However, if rates of net water entry (through the gills), and exit (through the kidney) were not in equilibrium, then the change in UFR may not accurately reflect the change in osmotic water permeability. The goal of this series was to address this issue by measuring changes in body mass. As any handling may alter water fluxes in fish, a paired design was employed where each fish served as its own control. Oscars (N=10) were acclimated to their chambers overnight, then anaesthetized as above, drained head-down in air for 15 s, patted thoroughly dry with soft towels, and weighed to 0.01 g accuracy. They were then returned to their chambers for a 6-h period of normoxia. The anaesthetization and weighing procedure was then repeated, and the change in body mass recorded. This protocol was duplicated in a second series with the same fish

(N=10) after a further 24 h of normoxia. The fish were again anaesthetized, and the initial mass was measured as before. However, the final mass was recorded after 3 h of normoxia plus 3 h of hypoxia, and the final anaesthetic solution was equilibrated to the hypoxic P_{O_2}. In each series, the change in body mass was expressed relative to the initial mass as g kg^{-1} of the initial mass.

Series 9

The objective of this final series was to look for possible changes in branchial surface morphology accompanying the changes in gill permeability seen during the normoxia–hypoxia–normoxic recovery regime in the preceding series. Oscars were allowed to settle in their chambers overnight, then killed under normoxia (N=6), and after 1 h of hypoxia (N=6), 3 h of hypoxia (N=6), 1 h of normoxic recovery (N=6) and 3 h of normoxic recovery (N=6). The fish were anaesthetized as above, and then killed by cephalic concussion. The second gill arch from the right hand side of each fish was excised, quickly rinsed in water, then immediately placed in cold Karnovsky's fixative for storage at 4°C. The samples were later shipped to San Diego State University, CA, USA, for examination by scanning electron microscopy.

Analytical techniques

Water P_{O_2} was routinely monitored using a portable O_2 probe and meter (WTW Oxi325 Oximeter, Weilheim, Germany). Water and urine total ammonia concentrations were measured colorimetrically by the salicylate hypochlorite assay (Verdouw et al., 1978). Na^+ and K^+ concentrations in water, plasma and urine were determined by flame atomic absorption spectrophotometry (AAnalyst 800, Perkin-Elmer, Wellesley, MA, USA). All radioactivity measurements (^{22}Na, ^3H_2O, [^{3}H]PEG-4000) were made by scintillation counting (LS6500, Beckman Coulter, Fullerton, CA, USA) on sample volumes of 5 ml for water, and 20–100 µl for plasma and urine, made up to 5 ml with water, added to 5 ml of Packard Ultima Gold AB Fluor (Perkin-Elmer, Wellesley, MA, USA). Internal standardization tests demonstrated that quenching was constant, so no correction was necessary. Urine flow rate (UFR) was determined gravimetrically.

Heart rate was measured using a Transmed 2991 impedance converter (Fullerton, CA, USA). Transepithelial potential (TEP) was measured by means of 3 mol l^{-1} KCl–agar bridges connected *via* Ag/AgCl electrodes (WPI, Sarasota, FL, USA) to a high impedance electrometer (Radiometer pHM 82 meter, Copenhagen, Denmark). The reference bridge was placed in the water in the fish chamber, and the measurement bridge was connected to the saline-filled intraperitoneal catheter. TEP measurements were expressed relative to the water side as 0 mV after correction for junction potential, which was less than 2 mV in all cases.

For gill morphology, the Karnovsky-fixed gill samples were rinsed in 0.1 mol l^{-1} phosphate-buffered saline (PBS), and post-fixed in 1% osmium tetroxide. The samples were then dehydrated in ascending concentrations of ethanol from 30%, concluding at 100%, critical-point-dried with liquid CO_2, mounted on the stubs and sputter-coated with gold for examination by scanning electron microscopy (SEM). The general structure of the gills and surface structure of the filamental and lamellar epithelia were examined with a Hitachi S 2700 scanning electron microscope (Tokyo, Japan) at an accelerating voltage of 20 kV. Morphometric quantification of mitochondria-rich cells (MRC) density (number of MRCs per mm^2 was performed on randomly selected areas of trailing edges of filaments behind the respiratory lamellae. SE micrographs (×2000 magnification) of five randomly selected areas of filament epithelium for each fish were analysed. The number of apical crypts of MRCs per unit area was counted. The individual surface areas of 30 MRCs were calculated on photographs at ×6000 magnification according to the shape of their two-dimensional apical openings, which varied from circular to oval, triangular and roughly trapezoidal.

Calculations

Net flux rates (in µmol kg^{-1} h^{-1}) of Na^+ (J^{Na}_{net}), K^+ and total ammonia were calculated from changes in concentration (in µmol l^{-1}), factored by the known fish mass (in kg), volume (in l), and time (in h). The traditional method for determining unidirectional Na^+ fluxes (Kirschner, 1970; Wood, 1992) is to measure influx (J^{Na}_{in}, by convention positive) directly as the disappearance of ^{22}Na radioactivity from the external water, and to calculate efflux (J^{Na}_{out}, by convention negative) as the difference, using the conservation equation:

$$J^{Na}_{in} + J^{Na}_{out} = J^{Na}_{net} . \quad (1)$$

In this method, which was used in Series 2, influx is calculated as:

$$J^{Na}_{in} = \frac{([CPM_i] - [CPM_f])\,(V)}{(SA_{ext})\,(t)\,(M)} , \quad (2)$$

where, CPM_i is the initial ^{22}Na radioactivity in the water (in c.p.m. l^{-1}) at the start of the flux period; CPM_f is the final ^{22}Na radioactivity in the water (in c.p.m. l^{-1}) at the end of the flux period; V is the volume of water (in l); SA_{ext} is the mean external specific activity (^{22}Na per total Na^+) in the water (in c.p.m. µmol^{-1}), calculated from measurements of water ^{22}Na radioactivity and total water $[Na^+]_{ext}$ at the start and end of the flux period; t is the time of flux period (in h); M is the mass of the fish (in kg).

However, it is also possible to measure Na^+ efflux directly by the appearance of ^{22}Na radioactivity in the external water, from the extracellular fluid of the fish. This approach is rarely used because it requires far more radioisotope, but was employed in Series 1 and 3.

In this method, efflux is calculated as:

$$J^{Na}_{out} = \frac{([CPM_i] - [CPM_f])\,(V)}{(SA_{int})\,(t)\,(M)} , \quad (3)$$

where, SA_{int} is the internal specific activity (^{22}Na per total Na^+) in the plasma of the fish (in c.p.m. µmol^{-1}). The other symbols are the same as in Eqn 2. SA_{int} was calculated from plasma ^{22}Na radioactivity and total $[Na^+]$ measured from the terminal blood sample. Sensitivity calculations, using the internal ^{22}Na space estimate for the rainbow trout (280 ml kg^{-1}) (Wood, 1988), demonstrated that the decline in SA_{int} as a result of the loss of ^{22}Na to the external water and urine over the 6-h (Series 3) to 9-h (Series 1) experiments would have caused less than a 5% fall in SA_{int}, and therefore negligible error in the calculation of J^{Na}_{out}, so no correction was made.

In Series 6, the rate constant of ^3H_2O efflux was calculated from the rate of decline in total ^3H_2O in the fish, which was approximately exponential with time (Evans, 1967):

$$k = \frac{(\ln CPM_1 - \ln CPM_2)}{(t_1 - t_2)} , \quad (4)$$

where, k is the rate constant of the efflux (in h^{-1}); CPM_1 is the total ^3H_2O radioactivity (in c.p.m.) in the fish at time t_1 (in h); CPM_2 is the total ^3H_2O radioactivity (in c.p.m.) in the fish at time t_2 (in h).

Absolute rates of diffusive water efflux were calculated as the product of k multiplied by the water space of the fish (assumed to be 800 ml kg^{-1}) (Holmes and Donaldson, 1971; Olson, 1992). In practice, water efflux rates were calculated for each 1-h period

of the experiment, by regressing the three measurements of *CPM* at 0, 0.5 and 1 h against time to yield the slope k. By measuring the ^{3}H in the water after 30 h, when complete equilibration between the fish and the water had occurred, it was possible to calculate accurately the total amount of radioactivity (CPM_{total}) in the system. The volume of the system was taken as the measured volume of external water plus the water space of the fish. Therefore, from CPM_{total} and from measurements of ^{3}H appearance in the water at each time interval, it was possible to keep track of *CPM* in the fish at each time during the experiment.

In Series 1, 2 and 7, urinary excretion rates (ER) were calculated as the product of urine flow rate (UFR) multiplied by the measured concentrations (e.g. Na^+, K^+, total ammonia, [^{3}H]PEG-4000) in the urine. In Series 7, the rate of clearance of [^{3}H]PEG-4000 across the gills and through the urine were calculated. As clearance rate represents the volume of plasma cleared per kg per h, the calculation requires an estimate of [^{3}H]PEG-4000 radioactivity in plasma at each time during the experiment. We assumed that this marker was distributed at plasma concentration in a space of 250 ml kg^{-1}, i.e. a volume chosen to approximate the extracellular space (Holmes and Donaldson, 1971; Olson, 1992). We calculated the total [^{3}H]PEG-4000 radioactivity in the fish at the end of the experiment as the product of this extracellular space multiplied by the final measured plasma concentration in the terminal blood sample. By keeping track of the total amount of [^{3}H]PEG-4000 radioactivity excreted into the water and in the urine in each flux period, we were able to calculate the amount present in the extracellular space at the beginning and end of each flux period, and therefore the average plasma concentration of [^{3}H]PEG-4000 during the flux period in question. Clearance rates (in ml plasma kg^{-1} h^{-1}) were then calculated as the amounts excreted through each route during the flux period, factored by the fish mass, time, and average plasma concentration:

$$\text{Gill [}^3\text{H]PEG-4000 clearance rate} = \frac{([CPM_f] - [CPM_i])\,(V)}{(CPM_p)\,(t)\,(M)}, \quad (5)$$

$$\text{Urinary [}^3\text{H]PEG-4000 clearance rate} = \text{GFR} = \frac{(\text{UFR})\,(CPM_u)}{CPM_p}, \quad (6)$$

where, CPM_f is the final [^{3}H]PEG-4000 radioactivity in the water (in c.p.m. l^{-1}) at the end of the flux period; CPM_i is the initial [^{3}H]PEG-4000 radioactivity in the water (in c.p.m. l^{-1}) at the start of the flux period; CPM_p is the average plasma [^{3}H]PEG-4000 radioactivity (in c.p.m. ml^{-1}) during the flux period; CPM_u is the urine [^{3}H]PEG-4000 radioactivity (in c.p.m. ml^{-1}) during the collection period; GFR is the glomerular filtration rate (in ml kg^{-1} h^{-1}); UFR is the urine flow rate (in ml kg^{-1} h^{-1}); The other symbols are the same as in Eqn 2.

In Series 7, urinary Na^+ and water handling (cf. Wood and Patrick, 1994) were assessed as:

$$FR_{Na} = (\text{GFR})\,([Na^+]_p) \quad (7)$$

$$ER_{Na} = (\text{UFR})\,([Na^+]_u) \quad (8)$$

$$RR_{Na} = FR_{Na} - ER_{Na} \quad (9)$$

$$CR_{Na} = (ER_{Na})\,(FR_{Na})^{-1} \quad (10)$$

$$CR_{H_2O} = (\text{UFR})\,(\text{GFR})^{-1}, \quad (11)$$

where, FR_{Na} is the filtration rate of Na^+ (in μmol kg^{-1} h^{-1}) at the glomeruli; ER_{Na} is the excretion rate of Na^+ (in μmol kg^{-1} h^{-1}) in the urine; RR_{Na} is the reabsorption rate of Na^+ (in μmol kg^{-1} h^{-1}) in the renal tubules; CR_{Na} is the clearance ratio of Na^+; CR_{H_2O} is the clearance ratio of water; $[Na^+]_p$ is the plasma Na^+ concentration; $[Na^+]_u$ is the urine Na^+ concentration.

All data have been reported as means ± 1 s.e.m. (*N*). Relationships were assessed by one-way ANOVA followed by the Bonferroni multiple comparison test for independent data, or Dunnett's multiple comparison test for paired data, as appropriate, to determine when values became significantly different from reference means. Student's two-tailed *t*-test was used for single comparisons. A significance level of $P \leq 0.05$ was used throughout.

RESULTS

Direct *versus* indirect measurements of J^{Na}_{out} and J^{Na}_{in} at the gills during hypoxia

Direct determinations of unidirectional Na^+ efflux by measurement of ^{22}Na appearance into the water from bladder-catheterized oscars (Series 1) demonstrated that J^{Na}_{out} was reduced during acute hypoxia, and that this occurred at the gills. The control rates under normoxia were approximately –350 μmol kg^{-1} h^{-1}. The decrease in J^{Na}_{out} became significant by the second hour of hypoxia and persisted through to the fourth hour, averaging about a 55% reduction (Fig. 1A). J^{Na}_{out} increased significantly during the first hour of normoxic recovery, returning immediately to the original normoxic control levels. J^{Na}_{net} (approximately –90 μmol kg^{-1} h^{-1}) did not change significantly during the regime relative to normoxic control levels, but became more negative than during hypoxia in the first hour of normoxic recovery (Fig. 1A). Measurements of J^{Na}_{net} and J^{Na}_{out} allowed calculation of J^{Na}_{in}, which showed similar trends to J^{Na}_{out} J^{Na}_{in}, approximately +260 μmol kg^{-1} h^{-1} under normoxia, declined significantly during acute hypoxia, the decreases becoming significant by the second hour and averaging about 70% through to the fourth hour (Fig. 1A). J^{Na}_{in} increased significantly upon re-institution of normoxia, returning to values not significantly different from the original control levels.

Direct determinations of J^{Na}_{in} by measurement of ^{22}Na disappearance from the water, using bladder-catheterized oscars (Series 2), produced data very similar to those reported earlier by Wood et al. (Wood et al., 2007) who studied oscars without bladder catheters (cf. Figs 1 and 2 of that publication). Therefore, the data are not reported in detail here. The data were also generally similar to those of Series 1 (cf. Fig. 1A) where J^{Na}_{out} was measured directly. In Series 2, directly measured J^{Na}_{in} fell by 80% and indirectly measured J^{Na}_{out} fell by 60% during acute hypoxia, without significant change in J^{Na}_{net}. The only substantive difference from the pattern of Fig. 1A was that directly measured J^{Na}_{in} remained significantly depressed during the first hour of normoxic recovery, but was restored during the second hour, in accord with the report of Wood et al. (Wood et al., 2007).

K^+ loss rates *via* the gills during hypoxia

Under normoxia, net K^+ loss rates *via* the gills in the bladder-catheterized oscars of Series 1 were approximately –45 μmol kg^{-1} h^{-1}, only about half those of Na^+ (Fig. 1B *versus* Fig. 1A). During acute hypoxia, K^+ loss rates decreased by about 55%, an effect that was significant during all four hours of exposure. Upon return to normoxia, K^+ loss rates increased significantly, returning to original control levels during the first hour of recovery. In Series 2 (data not shown), net K^+ loss rates fell from normoxic control values of –35.3±6.9 μmol kg^{-1} h^{-1} (*N*=6) to –18.2±9.8 μmol kg^{-1} h^{-1} (6) during hypoxia, and then returned to –31.1±10.5 μmol kg^{-1} h^{-1} (6) during the first hour of

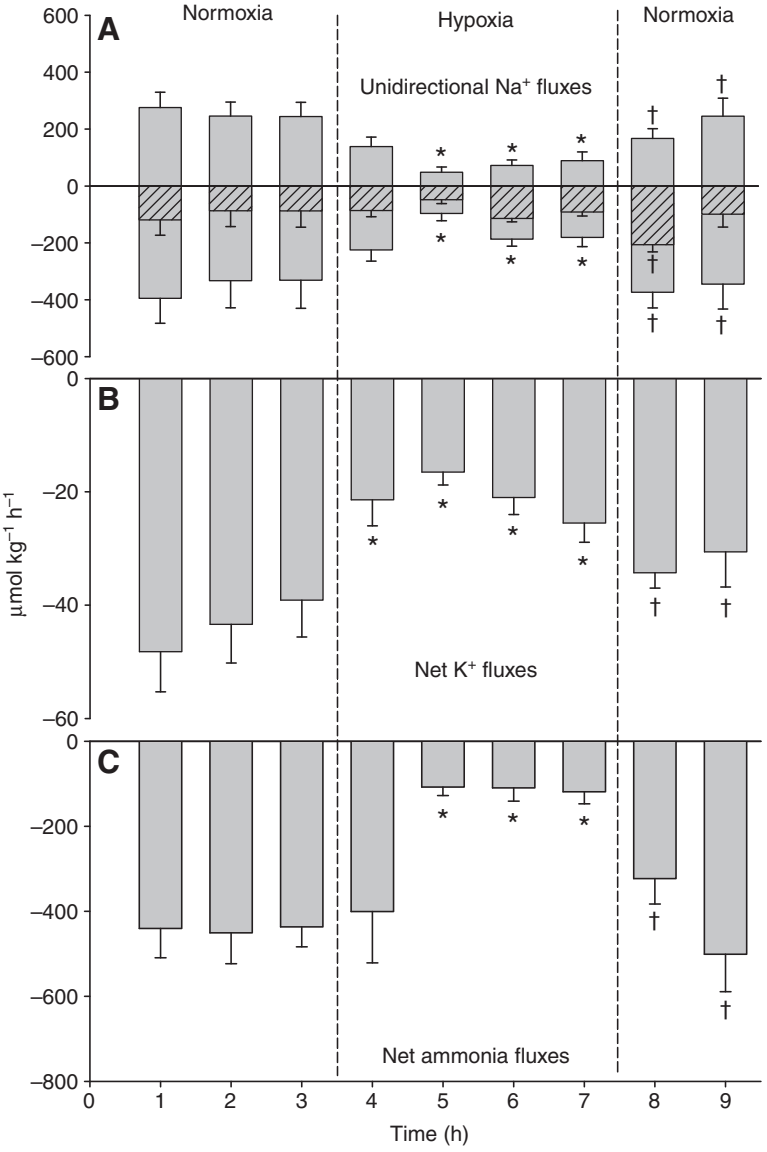

Fig. 1. (A) Changes in unidirectional (J^{Na}_{out}, J^{Na}_{in}) and net flux rates (J^{Na}_{net}) of Na^+ *via* the gills in oscars of Series 1 fitted with urinary bladder catheters. J^{Na}_{out} values are downward (negative) bars, J^{Na}_{in} values are upward (positive) bars, and J^{Na}_{net} values are hatched bars. J^{Na}_{out} and J^{Na}_{net} were measured directly, and J^{Na}_{in} was calculated using Eqn 1. The fish were exposed to a normoxia (P_{O_2}=130–150 torr) – acute hypoxia (P_{O_2}=10–20 torr) – normoxic recovery (P_{O_2}=130–150 torr) regime. (B,C) Changes in (B) the net flux rates of K^+ and (C) the net flux rates of ammonia *via* the gills during this same regime. Values are means ± 1 s.e.m. (N=7). *Significant difference ($P\leq0.05$) from the average rate during the 3-h normoxic control period; †significant difference ($P\leq0.05$) from the average rate during the final 3 h of the hypoxic period.

normoxic recovery, in a pattern comparable to that of Series 1 (cf. Fig. 1B).

Ammonia excretion rates *via* the gills during hypoxia

In Series 1, ammonia excretion rates were around –440 µmol kg^{-1} h^{-1} under control normoxic conditions, but declined markedly during hypoxia (Fig. 1C). There was no change in the first hour, but thereafter they stabilized at a 75% reduction through to the fourth hour. Ammonia excretion increased significantly during the first hour of normoxic recovery, returning to values not significantly different from the original control levels at this time. An almost identical pattern was seen in Series 2 (data not shown).

Urine flow rate and urinary excretion rates during hypoxia

The urine collections (combined data of Series 1 and 2) demonstrated that UFR, which was approximately 3 ml kg^{-1} h^{-1} under normoxic control conditions, fell by about 75% during hypoxia; the decrease became significant by the second hour of exposure, and remained significant in the first hour of normoxic recovery (Fig. 2A). Thereafter, UFR recovered and indeed rebounded above the original control rate during the following overnight collection, a period of about 12 h. In Series 1 the fish were handled (blood-sampled) before this second overnight collection, whereas in Series 2 the fish were not handled, but the overshoot occurred in both series, so the data were combined.

Urinary [Na^+] was about 11 mmol l^{-1} under normoxia, and tended to rise slightly during hypoxia, and decline during normoxic recovery but the changes were not significant (Fig. 2C). Therefore urinary Na^+ excretion rate (ER_{Na}) tended to track UFR, falling from control rates of approximately –33 µmol kg^{-1} h^{-1} under normoxia to –15 µmol kg^{-1} h^{-1} under hypoxia (Fig. 2B). The decreases in ER_{Na} were significant in the second and fourth hours of hypoxia, and the first hour of normoxic recovery. Thereafter, control rates of ER_{Na} were restored. Overall, urinary Na^+ losses (Fig. 2C) were only about 25% of the total, the other 75% occurring across the gills as J^{Na}_{net} (cf. Fig. 1A).

Urinary [ammonia] was less than 3 mmol l^{-1} and remained stable during hypoxia and normoxic recovery (Fig. 2C), so ER_{Amm} (Fig. 2B) directly tracked the changes in UFR (Fig. 2A). Excretion of ammonia through the urine was very low (about –7 µmol kg^{-1} h^{-1} under normoxia), averaging less than 2% of the excretion rate across the gills (cf. Fig. 1C).

Urinary [K^+] was not measured on all samples because of sample volume limitations. However, as for [Na^+] and [ammonia], urinary [K^+] appeared to remain stable [1.09±0.09 mmol l^{-1} (15) under normoxia *versus* 0.83±0.14 mmol l^{-1} (13) under hypoxia], so ER_K again appeared to track UFR, and amounted to only about 10% of net rate of K^+ loss across the gills (cf. Fig. 1B).

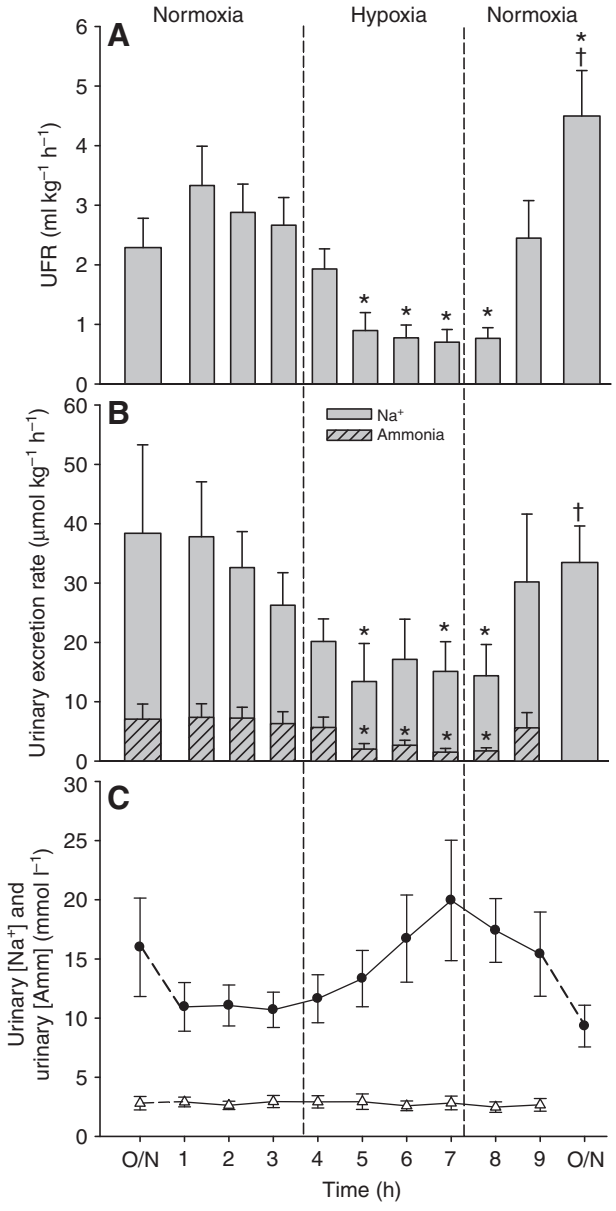

Fig. 2. Changes in (A) urine flow rate (UFR), (B) urinary excretion rates of Na^+ (shaded bars) and total ammonia (hatched bars), and (C) concentrations of Na^+ (solid circles) and total ammonia (open triangles) in the urine of oscars of Series 1 and 2, fitted with urinary bladder catheters. The fish were exposed to a normoxia (P_{O_2}=130–150 torr) – acute hypoxia (P_{O_2}=10–20 torr) – normoxic recovery (P_{O_2}=130–150 torr) regime. Values during the original overnight recovery period (O/N) following cannulation, and during the second overnight recovery period (O/N) following the hypoxic exposure regime are also shown. Urinary ammonia measurements were not made for the latter. Values are means ± 1 s.e.m. (N=17). *Significant difference ($P \leq 0.05$) from the average rate during the 3-h normoxic control period; †significant difference ($P \leq 0.05$) from the average rate during the final 3 h of the hypoxic period.

Lack of Na^+ exchange diffusion

When water [Na^+]$_{ext}$ was acutely increased from 135±2 μmol l^{-1} (7) to 1232±43 μmol l^{-1} (7) in bladder-catheterized oscars of Series 3, J_{in}^{Na} increased almost threefold in the expected fashion, but branchial J_{out}^{Na}, measured directly, did not change, so J_{net}^{Na} became positive (Fig. 3). Therefore the phenomenon of exchange diffusion, an obligatory 1:1 linkage of a portion of J_{out}^{Na} to J_{in}^{Na}, does not appear to occur in the gill Na^+ transport system of oscars.

Heart rates and breathing rates during hypoxia

In Series 4, heart rate fell significantly from about 66 beats min^{-1} to 38 beats min^{-1} within the first 5 min of acute hypoxia, and by 45 min had stabilized at approximately 31 beats min^{-1} (Fig. 4A). Upon re-institution of normoxia, heart rate increased to about 53 beats min^{-1} within 5 min, but full recovery to control normoxic rates took 45 min. Breathing rate was around 45 beats min^{-1} and did not change significantly during the exposure regime (Fig. 4B). However, by visual observation, breathing amplitude increased greatly during hypoxia and decreased during normoxic recovery.

Transepithelial potentials during hypoxia, and the response to water calcium

Transepithelial potential (TEP) was maintained at a stable value of about –31 mV under normoxia, but became less negative (–14 to –9 mV) during all 3 h of hypoxia in the oscars of Series 5 (Fig. 5A). Full recovery of control values occurred only after 2 h of restoration of normoxia. When the water calcium concentration ([Ca^{2+}]$_{ext}$) was increased under normoxia, TEP became progressively less negative in an approximately linear fashion with log [Ca^{2+}]$_{ext}$ (Fig. 5B). At 1000–3200 μmol Ca^{2+} l^{-1}, TEP values were not significantly different from 0 mV.

Diffusive exchange of water during hypoxia

Rate constants (k) of diffusive water exchange, measured with ^3H_2O in oscars of Series 6, were stable at 0.43±0.04 h^{-1} (9) during the 3-h normoxic control period, but fell progressively during acute hypoxia, reaching 0.12±0.01 h^{-1} (10) by the third hour of exposure. Recovery was virtually immediate, and control rates of 0.42±0.04 h^{-1} (8) were re-established within the first hour. These values of k

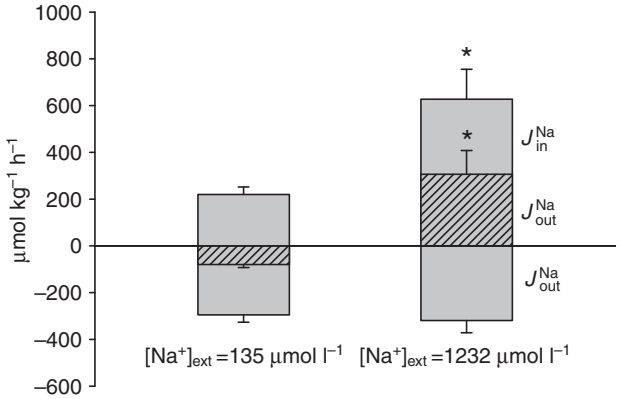

Fig. 3. The effect of an acute increase in water Na^+ concentration ([Na^+]$_{ext}$) from 135±2 μmol to 1232±43 μmol l^{-1} on unidirectional (J_{out}^{Na}, J_{in}^{Na}) and net flux rates (J_{net}^{Na}) of Na^+ *via* the gills in bladder-catheterized oscars of Series 3. J_{out}^{Na} values are downward (negative) bars, J_{in}^{Na} values are upward (positive) bars, and J_{net}^{Na} values are hatched bars. J_{out}^{Na} and J_{net}^{Na} were measured directly, and J_{in}^{Na} was calculated using Eqn 1. Values are means ± 1 s.e.m. (N=7). *Significant difference ($P \leq 0.05$).

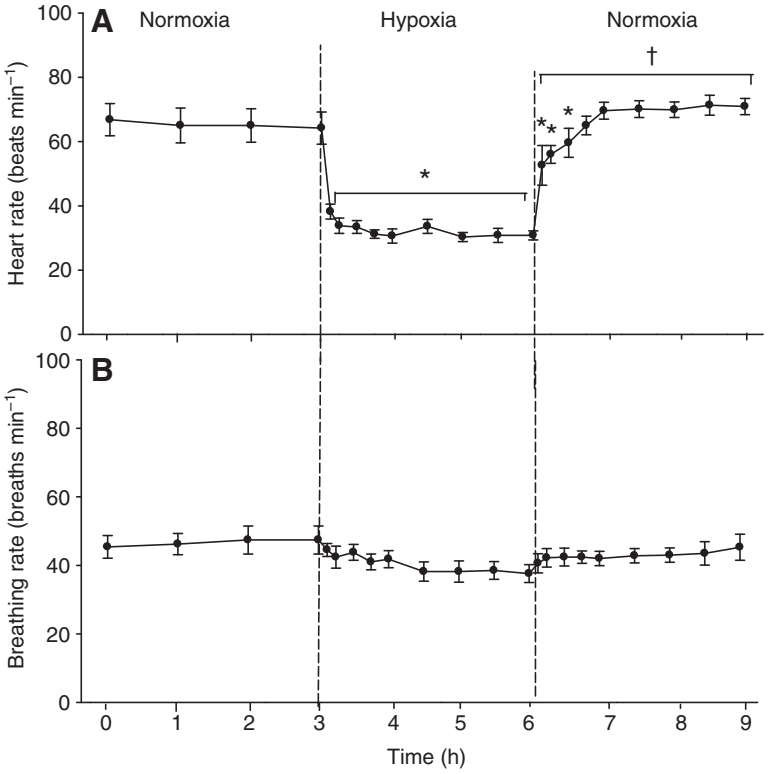

Fig. 4. Changes in (A) heart rate and (B) breathing rate in oscars of Series 4 exposed to a normoxia (P_{O_2}=130–150 torr) – acute hypoxia (P_{O_2}=10–20 torr) – normoxic recovery (P_{O_2}=130–150 torr) regime. Values are means ± 1 s.e.m. (N=5). *Significant difference ($P \leq 0.05$) from the average rate during the 3-h normoxic control period; †significant difference ($P \leq 0.05$) from the average rate during the final 2 h of the hypoxic period. There were no significant changes in breathing rate.

yielded the diffusive water efflux rates of Fig. 6, which ranged from about 320 ml kg^{-1} h^{-1} during normoxia down to 90 ml kg^{-1} h^{-1} during severe hypoxia. The decline during hypoxia was significant in the first hour, and reached approximately 70% by the third hour. Note that absolute values of diffusive water efflux (i.e. unidirectional diffusive efflux) were approximately 100-fold greater than of UFR (cf. Fig. 2A), which is an index of net osmotic water flux (see Discussion).

Clearance rates of [^{3}H]PEG-4000 *via* the gills during hypoxia

The rate of clearance of the paracellular permeability marker polyethylene glycol (M.W.=4000; [^{3}H]PEG-4000) across the gills in bladder-catheterized oscars of Series 7 did not change significantly during acute hypoxia or during normoxic recovery (Fig. 7). Gill clearance rates were extremely low, averaging only about 0.4 ml plasma kg^{-1} h^{-1}, or about 5% of the simultaneously measured clearance rate of [^{3}H]PEG-4000 *via* the urine (cf. Fig. 8A).

Glomerular filtration rate, urine flow rate, and renal Na^+ and water handling during hypoxia

Glomerular filtration rate (GFR) measured as the clearance rate of [^{3}H]PEG-4000 *via* the urine in bladder-catheterized oscars of Series 7, was stable at about 9 ml plasma kg^{-1} h^{-1} during normoxia, but fell greatly during hypoxia, the reduction reaching 70% by the third hour of exposure (Fig. 8A). Upon re-institution of normoxia, GFR recovered within the first hour to values that were not significantly different from the original control rates. UFR showed a very similar trend with marked reduction by the third hour of hypoxia, and recovery upon re-institution of normoxia (Fig. 8B). In general, this response in UFR was similar to that seen earlier (cf. Fig. 2A), although absolute rates were higher, and the recovery during normoxia more rapid; the latter may reflect the fact that Series 7 used a 3-h hypoxic exposure period, whereas Series 1 and 2 used a 4-h period. In Series 7, the 'deficit' in UFR relative to the control rate over 3 h of hypoxia was 10.75 ml kg^{-1}. In Series 8, measurements of changes in body mass demonstrated that oscars lost significantly less mass [–5.41±1.39 g kg^{-1} (10)] after 3 h of normoxia plus 3 h of hypoxia, than after 6 h of normoxia [–11.66±1.22 g kg^{-1} (10)]. Thus on a relative basis, fish gained 6.25 g kg^{-1} of water during hypoxia, accounting for 58% of the deficit (10.75 ml kg^{-1}) of UFR in Series 7. This observation was in accord with the subsequent overshoot in UFR recorded during overnight normoxic recovery in Series 1 and 2 (Fig. 2A).

Calculations of renal Na^+ handling (cf. Eqns 7–10) in Series 7, summarized in Table 1, demonstrated that tubular Na^+ reabsorption rate (RR_{Na}) closely tracked the glomerular filtration rate of Na^+ (FR_{Na}). Both fell greatly during hypoxia, and recovered upon return to normoxia. Urinary Na^+ excretion rate (ER_{Na}) also fell significantly during hypoxia, and recovered thereafter during normoxia (Table 1), in accord with the results of Series 1 and 2 (cf. Fig. 2B). Under normoxia, the clearance ratio for Na^+ was about 0.04, indicating highly efficient fractional reabsorption (96%), whereas that of water was about 0.61, indicating only 39% reabsorption. During hypoxia, the tubules became slightly less efficient at discriminating between Na^+ and water, as the Na^+ clearance ratio (CR_{Na}) doubled, indicating 92% reabsorption, whereas the clearance ratio of water (CR_{H_2O}; cf. Eqn 11) decreased slightly, indicating 46% reabsorption. These trends reversed during normoxic recovery (Table 1).

Surface morphology of the gills during hypoxia

In Series 9, scanning electron microscopy revealed a typical teleost gill structure with long filaments and well-defined respiratory lamellae. At a macro-level, this structure did not change during hypoxia and normoxic recovery, but there were pronounced changes in surface morphology. These changes were already substantial by 1 h of hypoxia, but even more pronounced by 3 h; they were partially reversed by 1 h of normoxic recovery, and fully reversed by 3 h. Under normoxia, there were abundant mitochondria rich cells

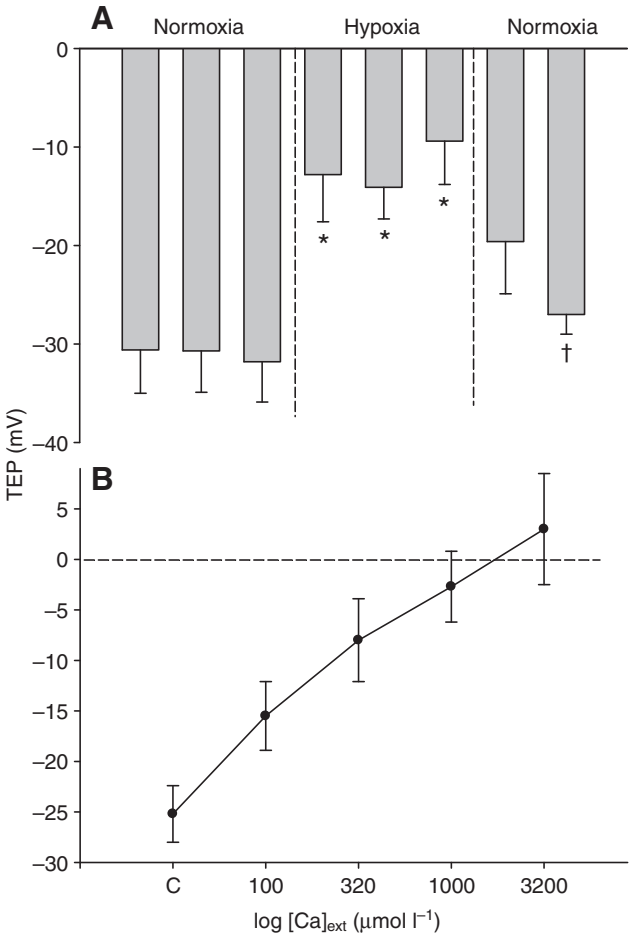

Fig. 5. (A) Changes in trans-epithelial potential (TEP) in oscars of Series 5 exposed to a normoxia (P_{O_2}=130–150 torr) – acute hypoxia (P_{O_2}=10–20 torr) – normoxic recovery (P_{O_2}=130–150 torr) regime. Values are means ± 1 s.e.m. (N=7). *Significant difference (P≤0.05) from the average value during the 3-h normoxic control period; †significant difference (P≤0.05) from the average value during the final 2 h of the hypoxic period. (B) The influence of increases in water calcium concentration ($[Ca^{2+}]_{ext}$) in half-logarithmic steps on TEP under normoxia. C is the background ($[Ca^{2+}]_{ext}$), nominally ~18 μmol l^{-1}. Values are means ± 1 s.e.m. (N=6).

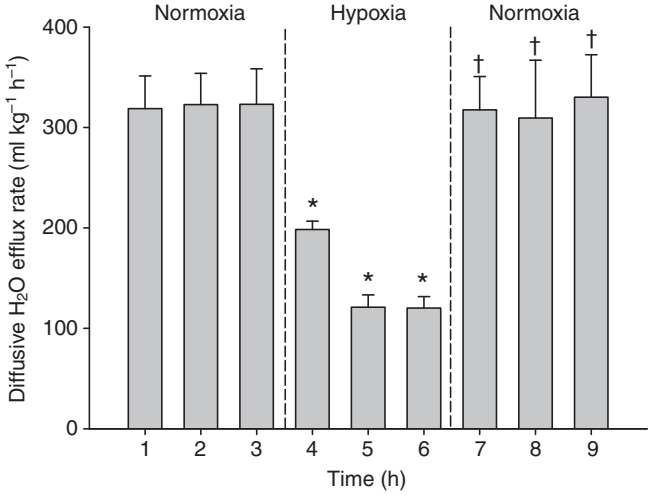

Fig. 6. Diffusive water efflux rates, measured with ^3H_2O in oscars of Series 6. The fish were exposed to a normoxia (P_{O_2}=130–150 torr) – acute hypoxia (P_{O_2}=10–20 torr) – normoxic recovery (P_{O_2}=130–150 torr) regime. Different sets of fish were used for each phase of the experiment (see Materials and Methods). Values are means ± 1 s.e.m. (N=9 during control normoxia, N=10 during hypoxia, and N=8 during hypoxic recovery). *Significant difference (P≤0.05) from the average rate during the 3-h normoxic control period; †significant difference (P≤0.05) from the average rate during the final 2 h of the hypoxic period.

(MRCs) on the trailing edges of the filaments and on the lamellae (Fig. 9A). The MRCs were recessed, opening to the surface by irregularly shaped apical crypts in between large pavement cells (PVCs) with complex surface patterns composed of numerous apical microridges (Fig. 9B). Occasional mucus cells (MCs) were visible, interdigitating between the PVCs. At higher magnification, typical apical crypts were relatively flat, and roughly trapezoid or triangular with a sieve-like surface structure composed of interdigitated and fused microplicae (Fig. 9C). During hypoxia, MRCs disappeared from the lamellar surface and became far less abundant on the filamental surface as many of the apical crypts closed (Fig. 9D). The remaining MRC crypts were much smaller, and more deeply recessed (Fig. 9E). PVC morphology was also altered, becoming simpler with a smooth central part and fewer concentric microridges concentrated at the outer edges of the cells, suggesting a stretching associated with covering of the crypts. At higher magnification, apical crypts of the MRCs were greatly reduced in surface area, and tended to be highly concave (Fig. 9F). However, MCs did not change their appearance.

Morphometric analysis of high power micrographs demonstrated that apparent MRC density (i.e. number of apical crypt openings per mm^2) on surfaces of the trailing edges of the filaments (about 1700 mm^{-2} under normoxia) fell significantly by 1 h, and was reduced by 47% after 3 h of hypoxia (Fig. 10A). Simultaneously, the average surface area of individual apical crypts, which was approximately 5.6 μm^2 under normoxia, declined by 65% during hypoxia (Fig. 10B). Thus total exposed MRC area on the filament surfaces declined by about 80% during hypoxia. By 1 h of return to normoxia, these effects were significantly reversed, and by 3 h, recovery of both MRC density (Fig. 10A) and apical crypt surface area (Fig. 10B) was complete.

DISCUSSION

A cost-saving strategy for adaptation to hypoxia

Direct measurements of ^{22}Na efflux in bladder-catheterized oscars (Series 1) confirmed that acute exposure to severe hypoxia causes a pronounced reduction of J_{out}^{Na} at the gills, as well as a large inhibition of J_{in}^{Na}, such that net Na^+ balance remains approximately constant (Fig. 1A). This is in accord with our earlier work, in which reciprocal methodology (direct measurement of J_{in}^{Na} by ^{22}Na disappearance from the water, indirect determination of J_{out}^{Na}) was employed, and urinary Na^+ efflux was not collected separately (Wood et al., 2007). Furthermore, the present Series 2 confirmed that prior anaesthesia with MS-222 and bladder catheterization did not alter the basic nature of the response. As the phenomenon of Na^+ exchange diffusion does not appear to be present in the gills of *Astronotus ocellatus* (Fig. 3), in contrast to approximately half of the Amazonian teleosts surveyed by Gonzalez et al. (Gonzalez et al., 2002), the downregulation of J_{out}^{Na} is not directly due to the reduction of J_{in}^{Na} *via* an obligatory 1:1 linkage. The two phenomena appear to be independent, which is also evidenced by the fact that in some individual fish J_{in}^{Na} was markedly reduced before J_{out}^{Na} (or *vice versa*) during hypoxia, and/or increased after J_{out}^{Na} during

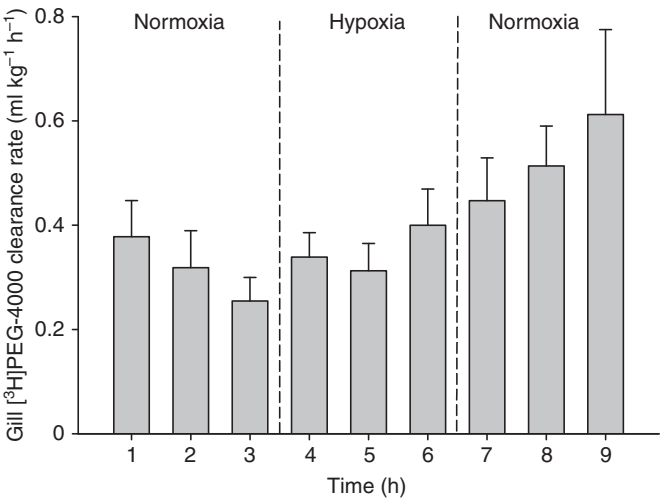

Fig. 7. Clearance rates of the paracellular marker radiolabelled polyethylene glycol (MW=4000; [^{3}H]PEG-4000) across the gills of oscars of Series 7, fitted with urinary bladder catheters. The fish were exposed to a normoxia (P_{O_2}=130–150 torr) – acute hypoxia (P_{O_2}=10–20 torr) – normoxic recovery (P_{O_2}=130–150 torr) regime. Values are means ± 1 s.e.m. (N=12). There were no significant differences (P≤0.05) during hypoxia or normoxic recovery from the average rate during the 3-h normoxic control period, and no significant differences (P≤0.05) during normoxic recovery from the average rate during the final 2 h of the hypoxic period.

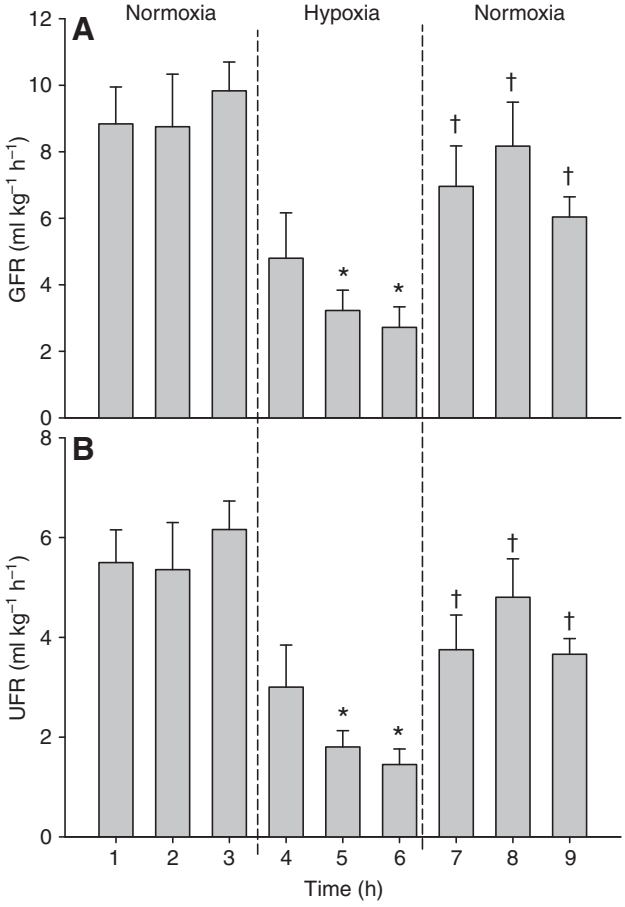

Fig. 8. Changes in (A) glomerular filtration rate (GFR), and (B) urine flow rate (UFR), measured as the urinary clearance rate of [^{3}H]PEG-4000, in oscars of Series 7 fitted with urinary bladder catheters. The fish were exposed to a normoxia (P_{O_2}=130–150 torr) – acute hypoxia (P_{O_2}=10–20 torr) – normoxic recovery (P_{O_2}=130–150 torr) regime. Values are means ± 1 s.e.m. (N=12). *Significant difference (P≤0.05) from the average value during the 3-h normoxic control period; †significant difference (P≤0.05) from the average value during the final 2 h of the hypoxic period.

normoxic recovery. These trends have also been seen in the overall means in some experimental series [e.g. figure 1B and figure 2B of Wood et al. (Wood et al., 2007), and Series 2 of the present study].

Whatever their causes, the advantages of these changes are obvious in a species that is routinely exposed to severe O_2 regimes that are inescapable and part of its normal lifestyle in the Amazon floodplain (Val and Almeida-Val, 1995). The cost of ionoregulation in freshwater fish has been estimated as 2–20% of resting metabolism (reviewed by Febry and Lutz, 1987), and direct measurements of O_2 consumption by perfused gills yield similar values (4–12%) (Wood et al., 1978; Lyndon, 1994; Morgan and Iwama, 1999). The ion-poor nature of Amazonian waters (Sioli, 1984) may exacerbate these costs, so at a time of severe O_2 limitation, it makes sense to turn down active ion uptake at the gills, as long as ion efflux can be similarly reduced. Dispersed gill cells of oscars appear to be perfectly capable of maintaining cellular O_2 uptake at P_{O_2}s even lower than used in the present study; indeed, even the P_{O_2} of expired water during severe hypoxia was higher than the levels that inhibited gill cell respiration (Scott et al., 2008). Therefore, reduction of active transport during hypoxia is probably a regulated phenomenon, rather than an automatic consequence of O_2 starvation. Indeed both Richards et al. (Richards et al., 2007) and Wood et al. (Wood et al., 2007) reported that gill Na^+/K^+-ATPase activity was downregulated by 60–65% after 3–4 h of severe hypoxia, and Lewis et al. (Lewis et al., 2007) noted a comparable decrease in gill protein synthesis rate.

The present results confirm that ion efflux rates at the gills are greatly reduced during severe hypoxia (Fig. 1A,B). Therefore plasma ion levels do not fall during hypoxia (Richards et al., 2007; Wood et al., 2007). In addition, ion loss rates through the urine are also decreased (Fig. 2B; Table 1), providing a smaller but still significant benefit. The larger cost-saving at the kidney may lie in the fact that Na^+ reabsorption rate in the kidney tubules, which is presumably active (Hickman and Trump, 1969; Wood and Patrick, 1994), is able to fall by 70% during hypoxia (Table 1) yet still achieve improved Na^+ conservation, thanks to the fact that glomerular filtration rate (Fig. 8A) and therefore filtered Na^+ load (Table 1) both decline so dramatically at this time.

Note that even during normoxia, these fasted oscars were in net negative Na^+ balance (Fig. 1A). Negative ion balance is typical of Amazonian fish in ion-poor native waters, and almost certainly the deficit is normally made up by electrolytes in the natural diet (Gonzalez et al., 2002; Gonzalez et al., 2005). The pellet diet which keeps these fish healthy in the lab contains substantial quantities of electrolytes (see Materials and methods).

Renal function during hypoxia

Renal function has not been assessed previously in *Astronotus ocellatus* or closely related species, but resting normoxic levels of GFR, UFR, and urinary Na^+ and ammonia excretion lie within the ranges reported for other freshwater teleosts (Hickman and Trump, 1969; Wood and Patrick, 1994). We are aware of only four previous studies on renal function during acute hypoxia in fish, all on the freshwater rainbow trout, and all showing exactly opposite trends to those in oscar – i.e. increased UFR and increased urinary Na^+

Table 1. Changes in renal Na^+ and water handling in oscars of Series 7 exposed to a normoxia – acute hypoxia – normoxic recovery regime

	Normoxia			Hypoxia			Normoxia recovery		
Time (h)	1	2	3	4	5	6	7	8	9
Na^+ filtration rate (FR_{Na}; μmol kg^{-1} h^{-1})	1219±156	1197±211	1366±142	633±169	450±87*	389±95*	951±168†	1100±150*	813±67*,†
Na^+ reabsorption rate (RR_{Na}; μmol kg^{-1} h^{-1})	1168±148	1144±200	1303±131	580±157	415±81*	359±91*	886±167†	1053±148†	773±63*,†
Na^+ excretion rate (ER_{Na}; μmol kg^{-1} h^{-1})	55±10	59±14	65±17	52±22	34±11*	30±9*	64±13†	52±8†	45±10
Na^+ clearance ratio‡ (CR_{Na})	0.04	0.05	0.05	0.08	0.08	0.08	0.07	0.05	0.05
H_2O clearance ratio‡ (CR_{H_2O})	0.62	0.61	0.62	0.63	0.56	0.53	0.54	0.58	0.60

Fish were exposed to normoxia (P_{O_2}=130–150 torr; hours 1–3) – acute hypoxia (P_{O_2}=10–20 torr; hours 4–6) – normoxic recovery (P_{O_2}=130–150 torr; hours 7–9).

Values are means ± 1 s.e.m., N=10–12.

*Significant difference (P≤0.05) for the average rate during the 3 h normoxic control period.

†Significant difference (P≤0.05) from the average rate during the final 2 h of the hypoxic period.

‡CR_{Na} and CR_{H_2O} were calculated from mean values using Eqns 10 and 11, respectively.

excretion rate (Hunn, 1969; Swift and Lloyd, 1974; Kobayashi and Wood, 1980; Tervonen et al., 2006). Tervonen et al. (Tervonen et al., 2006) implicated the mobilization of cardiac natriuretic peptide in the hypoxia-induced diuresis. Although GFR was not measured in any of these investigations, the responses were probably analogous to the situation during exercise in trout, where GFR and UFR increase in parallel and urinary Na^+ excretion rises (Wood and Randall, 1973b; Hofmann and Butler, 1979). These responses to exercise were attributed to the traditional osmorespiratory compromise – i.e. increased osmotic water entry at the gills accompanying increased $\dot{M}_{O_2}$. By contrast, the decrease in both GFR (Fig. 8A) and UFR (Fig. 8B) during acute hypoxia in the oscar appears to be facilitated in part by a reduction in the rate of osmotic water entry at the gills, but this is not the complete explanation. UFR declined by 70% during hypoxia in both Series 2 and 3 (Fig. 2A) and in Series 7 (Fig. 8B). The measurements of mass gain during hypoxia in Series 9 indicated that only about 42% of the reduction in UFR during hypoxia was actually due to decreased osmotic water entry, the remainder representing water that accumulated in the fish as a result of the reduction in GFR. This accumulated water was subsequently cleared by the overshoot in UFR during overnight normoxic recovery (Fig. 2A). Thus the rate of osmotic water entry fell by only 30% during hypoxia, while the GFR and UFR declines were both greater. Hypoxia is known to alter organ blood flow distribution (Schwerte et al., 2003) so the decline in GFR may reflect a fall in kidney perfusion. This can be viewed as another cost-saving measure, minimizing workloads of both the cardiovascular system and tubular Na^+ reabsorption (Table 1), as argued previously. Interestingly, Na^+ reabsorption and the discrimination between Na^+ and H_2O reabsorption became slightly less efficient, as indicated by the clearance ratio analysis of Table 1. This may reflect direct effects of low blood P_{O_2}s on tubular reabsorption processes (Epstein et al., 1994).

Heart rate changes during hypoxia

In common with virtually all other teleosts, oscars exhibited a profound bradycardia during hypoxia (Fig. 4A). This is undoubtedly of vagal origin. The adaptive significance of the response remains controversial, but most interpretations relate to either protecting cardiac function in the face of low P_{O_2} or a change in pattern of blood flow and/or pressure at the gills so as to improve the efficiency of respiratory gas exchange (reviewed by Sollid and Nilsson, 2006; Farrell, 2007). The latter is in accord with the increased branchial O_2 transfer factor down to a P_{O_2} of 20 torr with a return to normoxic levels at 10 torr reported by Scott et al. (Scott et al., 2008) in hypoxic oscars. None of the interpretations offered for bradycardia suggest that gas exchange efficiency is reduced, so this is unlikely to be the cause of the observed changes in gill permeability to ions and water.

How are oscars able to turn down gill ionic and osmotic permeability during hypoxia?

Permeability regulation at the gills of oscars during hypoxia is very different from the traditional osmorespiratory during exercise. It could be argued that this is because the gas exchange situation is different. $\dot{M}_{O_2}$ declines during hypoxia (e.g. Muusze et al., 1998; Sloman et al., 2006; Scott et al., 2008) but increases greatly during exercise. However branchial O_2 transfer factor does not fall during acute hypoxia (Scott et al., 2008). Furthermore, Lewis et al. (Lewis et al., 2007) reported that during normoxic recovery from an acute hypoxic exposure very similar to that used here, oscars exhibited a 270% overshoot in $\dot{M}_{O_2}$ relative to control levels, yet there was no elevation of ion loss rates (Fig. 1) or water exchange rates (Fig. 6) above control levels at this time in the present study (Fig. 1). So how are oscars able to turn down gill ionic and osmotic permeability during hypoxia without impeding respiratory gas exchange?

At a simpler level, we can ask whether this branchial permeability reduction is a transcellular or paracellular event. The various marker substances and experimental approaches used in this study cast some light on this issue, and with one exception (transepithelial potential), they point clearly to the former – a regulated reduction in transcellular permeability by 50–80%.

K^+ loss rates, which fell markedly during hypoxia, and recovered during normoxic restoration (Fig. 1B) are one such indicator. Because K^+ concentrations inside cells are about 100-fold greater than those in blood plasma, Lauren and McDonald (Lauren and McDonald, 1985) argued that K^+ loss rates at the gills of freshwater fish mainly reflect transcellular permeability. Had the gill cells become depolarized during hypoxia, increased K^+ leakage into the water would have been expected (Boutilier, 2001), but this did not occur.

Ammonia efflux rates (Fig. 1C), which followed a comparable pattern of reduction during hypoxia (Fig. 1C), are another such indicator. Note that plasma total ammonia levels increased during this hypoxic regime, so this was not driven by decreased internal ammonia levels (Wood et al., 2007). Although the exact mechanism(s) of ammonia efflux across the gills remains controversial, all models propose a transcellular route (cf. Wilkie, 2002). Recent findings that Rh glycoproteins in the gill cell membranes are central to the process (Nakata et al., 2007; Nawata et al., 2007) reinforce this conclusion. The situation is slightly

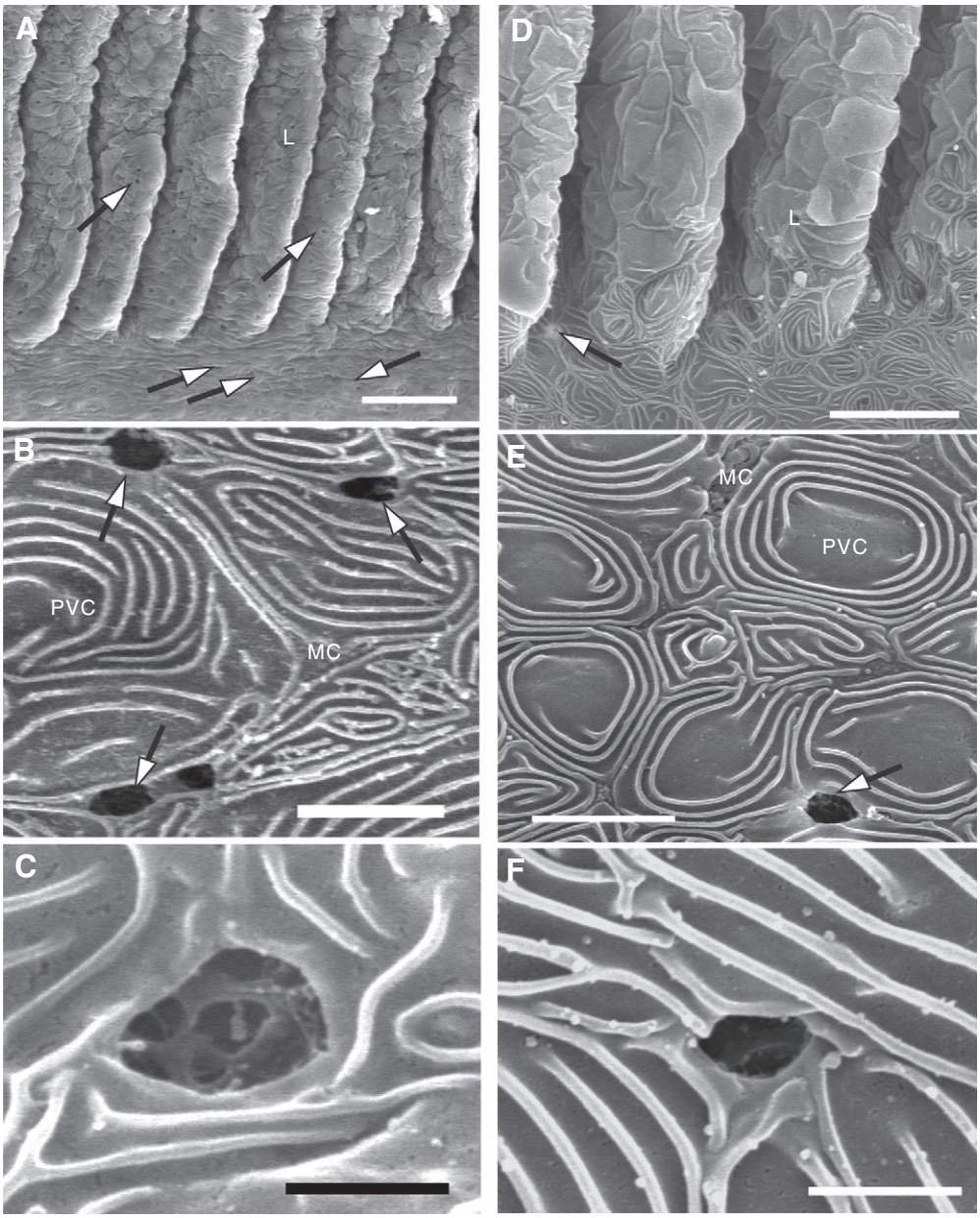

Fig. 9. Representative scanning electron micrographs of gill surfaces of oscars of Series 9 exposed to (A–C) normoxia (P_{O_2}=130–150 torr) or (D–F) 3 h of acute hypoxia (P_{O_2}=10–20 torr). (A,D) Low magnification views of the trailing edge of filament and lamellae (L). Under normoxia (A), note the abundance of mitochondria-rich cells (MRCs; arrows) on the filament and lamellae. Scale bar, 50 μm. Under hypoxia (D), note the reduced abundance of MRCs on the filamental surface, and the lack of visible MRCs on the lamellar epithelium. Scale bar, 25 μm. (B,E) Higher magnification view of the surface of the trailing edge of filament. Under normoxia (B), note large pavement cells (PVCs) with complex surface pattern composed of numerous microridges and irregularly shaped apical crypts of MRCs. A mucus cell (MC) is also visible. Scale bar, 10 μm. Under hypoxia (E), note the more simple pattern of the PVCs surface with a smooth central part and few concentric microridges on the edge of the cell, and reduced size of apical crypts of the MRC. An MC is again visible. Scale bar, 10 μm. (C,F) High magnification views of apical crypts of MRCs. Under normoxia (C), typical apical crypt is large, relatively flat, roughly trapezoid or triangular with a sieve-like surface structure composed of interdigitated and fused microplicae. Under hypoxia (F), the apical crypt surface area is greatly reduced and tends to be highly concave. Scale bars, 2 μm.

complicated by the fact that there is an apparent coupling of ammonia efflux to J_{in}^{Na} during normoxia in oscars, but this linkage is lost during hypoxia (Wood et al., 2007). Ammonia production rates may also decline during hypoxia (van den Thillart and Kesbeke, 1978; van Waarde, 1983), but since plasma total ammonia levels increase, ammonia excretion rate must be inhibited to a greater extent than production rate.

There was a marked attenuation of the negative TEP during hypoxia (Fig. 5A). Our original rationale in monitoring TEP was to use it as an indicator of paracellular permeabity changes, because the traditional interpretation of the TEP in freshwater teleosts is that it is a diffusion potential caused by the differential permeability of the gills to Na^+ *versus* Cl^- (Potts, 1984). The typical modulating effect of increasing $[Ca^{2+}]_{ext}$ (Fig. 5B), which has been seen in at least one other Amazonian fish (Wood et al., 1998) and many temperate freshwater teleosts (Eddy, 1975; McWilliams and Potts, 1978; Wood and Grosell, 2008) is attributed to the ability of divalent Ca^{2+} to 'tighten' the epithelium. The default assumption has always been that these effects occur at the paracellular pathway junctions, but we are aware of no definitive evidence that this is the case. Indeed, McDonald and Rogano (McDonald and Rogano, 1986) reported that whereas higher water $[Ca^{2+}]_{ext}$ greatly reduced Na^+ fluxes, it did not alter the clearance rate of the paracellular marker mannitol across the gills of freshwater trout. If indeed the bulk of Na^+ leakage occurs through the cell membranes of the branchial epithelium, then the 'tightening effects' of both hypoxia and $[Ca^{2+}]_{ext}$ may instead be operating on transcellular membrane channels.

Diffusive water efflux rate constants (k) measured with ^3H_2O (about 0.43 h^{-1} during normoxia), were generally very low in comparison to other teleosts, and close to those measured in the semi-terrestrial lungfish (reviewed by Patel et al., 2009). This fits with the general conclusion that gill permeability is low to start with in oscars as an adaptation to their challenging environment (Wood et al., 2007). The 70% reduction in k values and diffusive water efflux rates during hypoxia, and their rapid recovery during

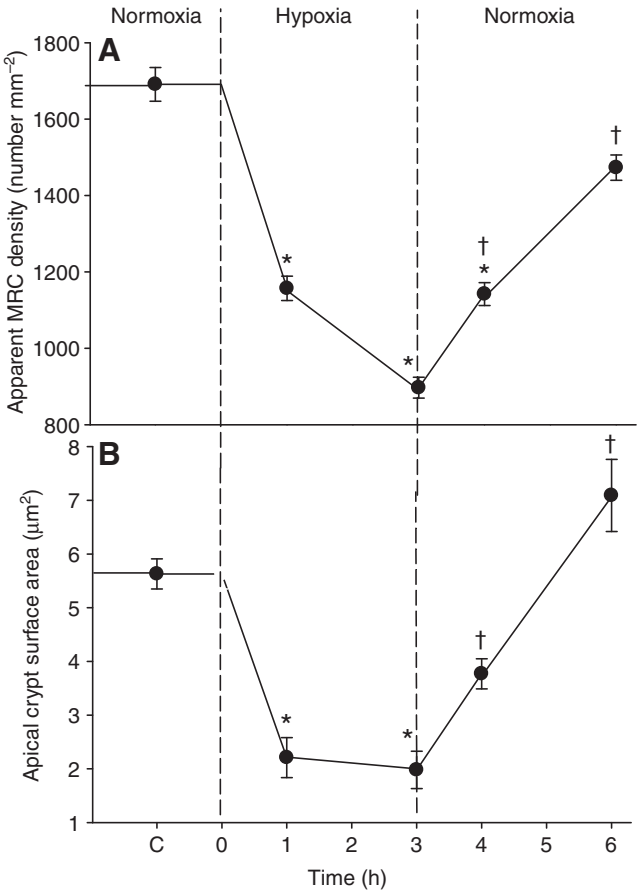

Fig. 10. Morphometric analysis of changes in gill surface morphology of oscars of Series 9 exposed to a normoxia (P_{O_2}=130–150 torr) – acute hypoxia (P_{O_2}=10–20 torr) – normoxic recovery (P_{O_2}=130–150 torr) regime. (A) The apparent density (i.e. number of apical crypt openings per mm^2) of mitochondria rich cells (MRCs) on surfaces of the trailing edges of the gill filaments. (B) The average surface area of individual apical crypts. Values are means ± 1 s.e.m. (N=6). *Significant difference (P≤0.05) from the control value (C) during normoxia; †significant difference (P≤0.05) from the value after 3 h of hypoxia.

restoration of normoxia (Fig. 6), when compared with UFR data (Fig. 2A, Fig. 8B) point to transcellular regulation. Diffusive water flux at fish gills is generally considered to occur by the transcellular route (Isaia, 1984; McDonald et al., 1991). The present results are very different from those of Loretz (Loretz, 1979) working on goldfish, who found a pronounced increase in diffusive water exchange during a much less severe hypoxia, in accord with the prediction of the traditional osmorespiratory compromise (Randall et al., 1972; Nilsson, 2007). They also differ from those of McDonald et al. (McDonald et al., 1991) who reported marked increases in diffusive water fluxes in rainbow trout, yellow perch, and smallmouth bass subjected to confinement stress.

By reasonable estimate of internal (300 mOsm) and external (2 mosmol) osmolarity, and the calculation approach developed by Potts et al. (Potts et al., 1967), it is possible to estimate the net diffusive water flux from the data of Fig. 6. This is about 0.53% of the unidirectional efflux rates or about 1.70 ml kg^{-1} h^{-1} during normoxia, falling to 0.51 ml kg^{-1} h^{-1} after 3 h of hypoxia. UFRs, the traditional measure of net osmotic water flux (Isaia, 1984), are about 1.7–2.9-fold higher than these values. This ratio is very typical for freshwater teleost fish. Isaia (Isaia, 1984) summarized comparable calculations for four freshwater teleosts (trout, eel, goldfish and flounder) yielding a mean ratio of 2.75 (range 2.1–3.3). This modest discrepancy has been recognized for many years and reflects the idea that diffusive water exchange mainly occurs through the cell membrane in freshwater teleosts, whereas osmotic water flux may additionally involve bulk flow through 'pores' or paracellular channels (Potts et al., 1967; Evans, 1969; Motais et al., 1969; Loretz, 1979; Isaia, 1984). As calculated earlier from the UFR and weight gain data, osmotic permeability (transcellular plus paracellular flux) in the oscar fell by only 30% during hypoxia, while diffusive water permeability (mainly transcellular flux) fell by 70%. The implication is that most of the reduction was in the transcellular component.

The branchial [^{3}H]PEG-4000 clearance data (Fig. 7) provide the most compelling evidence that gill permeability in hypoxic oscars is downregulated at a transcellular rather than a paracellular level. It is most unlikely that this large, uncharged molecule would move through cell membranes, and for this reason it has often been used successfully as an extracellular space marker (Munger et al., 1991; Olson, 1992) and gill paracellular permeability marker (Curtis and Wood, 1991; Kelly and Wood, 2002; Scott et al., 2004) in teleost fish. The present results (Fig. 7) demonstrate that gill paracellular permeability to PEG-4000 does not change during hypoxia. However, given the diversity of tight junction proteins, it remains possible that a single molecule such as PEG-4000 may not serve as a faithful marker for all paracellular fluxes. For example, a particular tight junction protein might regulate paracellular Na^+ flux more than paracellular Cl^- flux; this is an important area for future investigation. It is also noteworthy that gill [^{3}H]PEG-4000 clearance rates in oscar (0.3–0.6 ml plasma kg^{-1} h^{-1}; Fig. 7) are lower than in other freshwater teleosts such as trout (0.7–1.2 ml plasma kg^{-1} h^{-1}) (Curtis and Wood, 1991) and killifish (1.3–4.3 ml plasma kg^{-1} h^{-1}) (Scott et al., 2004), again pointing to generally low gill permeability in *Astronotus ocellatus*.

We propose that the reduction in gill transcellular permeability during acute hypoxia in the oscar is caused by the effective closure of membrane channels in the gill epithelial cells. This would conserve both ions and energy as outlined above. This idea is reminiscent of the 'channel arrest' hypothesis proposed to explain survival of the brain and liver in other severely hypoxia-tolerant organisms such as turtles and Crucian carp (Hochachka, 1986; Boutilier, 2001; Boutilier and St-Pierre, 2001; Hochachka and Lutz, 2001).

An obvious question is the nature of the channels that are effectively closed. We speculate that they are in fact a wide variety of channels – e.g. aquaporins for water (Evans et al., 2005), Rh proteins for ammonia (Nakada et al., 2007; Nawata et al., 2007), UT proteins for urea (McDonald et al., 2006), and potassium channels for K^+ (Boutilier, 2001; Boutilier and St-Pierre, 2001). The nature of the Na^+ channel is particularly interesting. Although most models of Na^+ uptake in freshwater fish incorporate an epithelial Na^+ channel (e.g. Evans et al., 2005; Marshall and Grosell, 2006), it has never been found at a genomic level. Regardless, since exchange diffusion of Na^+ is absent in *Astronotus ocellatus* and the reduction in Na^+ efflux appears not to be directly linked to the reduction in Na^+ influx during hypoxia, then the 'Na^+ channels' involved must be different from the ones contributing to Na^+ uptake. How does hypoxia close so many different channels? It is possible that the channels actually close individually or are removed at the level of the lipoprotein bilayer, but there may be a simpler explanation as outlined below, which does not require that all the channels be O_2-sensitive by themselves.

Morphological correlates of the channel arrest hypothesis

Unlike several other hypoxia-tolerant species, such as the Crucian carp (Sollid et al., 2003; Sollid et al., 2005; Sollid and Nilsson, 2006) goldfish (Sollid et al., 2005), and naked carp (Matey et al., 2008), the oscar did not exhibit 'remodelling' of the gill macrostructure during hypoxia. In the carp and goldfish, the gills actually gained surface area by losing inter-lamellar masses during hypoxia, whereas we had suspected that the opposite might occur in the oscar. Although it did not, it is possible that such alterations might have been seen had the duration of hypoxic exposure been longer. Nevertheless, we believe that the rapid and dramatic changes in gill surface morphology recorded during acute hypoxia may represent the morphological correlate of the channel arrest hypothesis. The 55–75% decreases in fluxes of Na^+, K^+, ammonia and water may be explained by the approximately 80% decrease in exposed MRC surface area, most of which occurred after only 1 h (Fig. 10). Apparently, this occurred by PVCs covering them. Generally low branchial flux rates of all substances in the oscar may be explained by the fact that the MRCs open only through small apical crypts, in contrast to much more extensive surface exposure in species such as trout (Goss et al., 1995; Goss et al., 1998). Indeed, one of the tenets of the channel arrest hypothesis is that effective ion channel densities should be inherently lower in hypoxia-tolerant animals (Hochachka, 1986; Boutilier, 2001). In the case of the gills of oscar, only small changes in PVC coverage are needed to effect closure of apical crypts. This interpretation assumes that the MRCs, not the PVCs are the sites of these transcellular fluxes in the oscar. Although this idea is unusual, to our knowledge, there is as yet no definitive evidence apportioning transcellular fluxes in a quantitative manner between MRCs and PVCs in any freshwater teleost fish. However, it now seems to be widely accepted that changes in coverage of the MRCs by PVCs plays a large role in ion and acid–base fluxes responsible for correction of systemic pH disturbances (Goss et al., 1995; Goss et al., 1998). Our argument, in the case of the oscar, is that comparable coverage plays an important role in the rapid change in transcellular fluxes which occur during acute hypoxia. In future, more extensive examination of MRC and PVC fine structure in the gills of normoxic and hypoxic oscars, using transmission electron microscopy, coupled with autoradiography to pinpoint the location of labelled markers, may cast light on this idea.

This work was funded by a NSERC Discovery Grant to C.M.W., and a National Research Council (CNPq) of Brazil/Amazon State Research Foundation (FAPEAM) PRONEX grant to A.L.V. C.M.W. is supported by the Canada Research Chair Program, and his travel was funded in part by the International Congress of Comparative Physiology and Biochemistry. A.L.V. and V.M.F.A.V. are recipients of research fellowships from CNPq. K.A.S. was supported by a grant from the Association for the Study of Animal Behaviour and the Royal Society (UK). G.D.B. was supported by a grant from the Research Foundation of Flanders (FWO). G.R.S. was supported by an Izaak Walton Killam Predoctoral Fellowship and was the recipient of a JEB travelling fellowship. F.X.V.D. was recipient of a fellowship from PIATAM/FINEP and R.M.D. is a recipient of a fellowship from CNPq. We thank Steve Perry and two anonymous reviewers for constructive comments, Maria de Nazaré Paula da Silva, Richard Sloman Sunita Nadella, and Daiani Kochann for excellent technical assistance, and all members of the Val lab for their hospitality.

REFERENCES

Almeida-Val, V. M. F. and Hochachka, P. W. (1995). Air-breathing fishes: metabolic biochemistry of the first diving vertebrates. In *Environmental and Ecological Biochemistry* (ed P. W. Hochachka and T. P. Mommsen), pp. 45-55. Amsterdam: Elsevier.

Almeida-Val, V. M. F., Val, A. L., Duncan, W. P., Souza, F. C. A., Paula-Silva, M. N. and Land, S. (2000). Scaling effects on hypoxia tolerance in the Amazon fish *Astronotus ocellatus* (Perciformes: Cichlidae): contribution of tissue enzyme levels. *Comp. Biochem. Physiol. B* **125**, 219-226.

Beyenbach, K. W. and Kirschner, L. B. (1976). The unreliability of mammalian glomerular markers in teleostean renal studies. *J. Exp. Biol.* **64**, 369-378.

Boutilier, R. G. (2001). Mechanisms of cell survival in hypoxia and hypothermia. *J. Exp. Biol.* **204**, 3171-3181.

Boutilier, R. G. and St-Pierre, J. (2000). Surviving hypoxia without really dying. *Comp. Biochem. Physiol. A* **126**, 481-490.

Curtis, B. J. and Wood, C. M. (1991). The function of the urinary bladder *in vivo* in the freshwater rainbow trout. *J. Exp. Biol.* **155**, 567-583.

Eddy, F. B. (1975). The effect of calcium on gill potentials and on sodium and chloride fluxes in the goldfish, *Carassius auratus*. *J. Comp. Physiol.* **96**, 131-142.

Epstein, F. H., Agmon, Y. and Brezis, M. (1994). Physiology of renal hypoxia. *Ann. N. Y. Acad. Sci.* **718**, 72-80.

Evans, D. H. (1967). Sodium, chloride, and water balance of the intertidal teleost, *Xiphister atropurpureus*. III. The roles of simple diffusion, exchange diffusion, osmosis and active transport. *J. Exp. Biol.* **47**, 525-534.

Evans, D. H. (1969). Studies on the permeability of selected marine, freshwater and euryhaline teleosts. *J. Exp. Biol.* **50**, 689-703.

Evans, D. H., Piermarini, P. M. and Choe, K. P. (2005). The multifunctional fish gill: dominant site of gas exchange, osmoregulation, acid–base regulation, and excretion of nitrogenous waste. *Physiol. Rev.* **85**, 97-177.

Farrell, A. P. (2007). Tribute to P. L. Lutz: a message from the heart: why hypoxic bradycardia in fishes? *J. Exp. Biol.* **210**, 1715-1725.

Febry, R. and Lutz, P. (1987). Energy partitioning in fish: the activity-related cost of osmoregulation in a euryhaline cichlid. *J. Exp. Biol.* **128**, 63-85.

Gonzalez, R. J. and McDonald, D. G. (1992). The relationship between oxygen consumption and ion loss in a freshwater fish. *J. Exp. Biol.* **163**, 317-332.

Gonzalez, R. J. and McDonald, D. G. (1994). The relationship between oxygen uptake and ion loss in fish from diverse habitats. *J. Exp. Biol.* **190**, 95-108.

Gonzalez, R. J., Wilson, R. W., Wood, C. M., Patrick, M. L. and Val, A. L. (2002). Diverse strategies for ion regulation in fish collected from the ion-poor, acidic Rio Negro. *Physiol. Biochem. Zool.* **75**, 37-47.

Gonzalez, R. J., Wilson, R. W. and Wood, C. M. (2005). Ionoregulation in tropical fish from ion-poor, acidic blackwaters. In *Fish Physiology*, vol. 22 (ed. A. L. Val, V. M. F. Almeida-Val and D. J. Randall), pp. 397-437. San Diego, CA: Academic Press.

Goss, G. G., Perry, S. F. and Laurent, P. (1995). Ultrastructural and morphometric studies on ion and acid–base transport processes in freshwater fish. In *Fish Physiology,* vol. 14 (ed. C. M. Wood and T. J. Shuttleworth), pp. 257-283. New York: Academic Press.

Goss, G. G., Perry, S. F., Fryer, J. N. and Laurent, P. (1998). Gill morphology and acid–base regulation in freshwater fishes. *Comp. Biochem. Physiol.* **119A**, 107-115.

Greco, A. M., Gilmour, K. M., Fenwick, J. C. and Perry, S. F. (1995). The effects of softwater acclimation on respiratory gas transfer in the rainbow trout *Oncorhynchus mykiss*. *J. Exp. Biol.* **198**, 2557-2567.

Greco, A. M., Fenwick, J. C. and Perry, S. F. (1996). The effects of soft-water acclimation on gill structure in the rainbow trout *Oncorhynchus mykiss*. *Cell Tissue Res.* **285**, 75-82.

Henriksson, P., Mandic, M. and Richards, J. G. (2008). The osmorespiratory compromise in sculpins: impaired gas exchange is associated with freshwater tolerance. *Physiol. Biochem. Zool.* **81**, 310-319.

Hickman, C. and Trump, B. (1969). Kidney. In *Fish Physiology*, vol. 1 (ed. W. S. Hoar and D. J. Randall), pp. 211-212. New York: Academic Press.

Hochachka, P. W. (1986). Defense strategies against hypoxia and hypothermia. *Science* **231**, 234-241.

Hochachka, P. W. and Lutz, P. L. (2001). Mechanism, origin, and evolution of anoxia tolerance in animals. *Comp. Biochem. Physiol. B* **130**, 435-459.

Hofmann, E. L. and Butler, D. G. (1979). The effect of increased metabolic rate on renal function in the rainbow trout, *Salmo gairdneri*. *J. Exp. Biol.* **82,** 11-23.

Holeton, G. F. and Randall, D. J. (1967). The effect of hypoxia upon the partial pressure of gases in the blood and water afferent and efferent to the gills of rainbow trout. *J. Exp. Biol.* **46**, 317-327.

Holmes, W. N. and Donaldson, E. M. (1969). The body compartments and the distribution of electrolytes. In *Fish Physiology,* vol. 1 (ed. W. S. Hoar and D. J. Randall), pp. 1-89. New York: Academic Press.

Hunn, J. B. (1969). Chemical composition of rainbow trout urine following acute hypoxic stress. *Trans. Am. Fish. Soc.* **98**, 20-22.

Isaia, J. (1984). Water and nonelectrolyte permeation. In *Fish Physiology*, vol. 10B (ed. W. S. Hoar and D. J. Randall), pp. 1-38. New York: Academic Press.

Kelly, S. P. and Wood, C. M. (2002). Cultured gill epithelia from freshwater tilapia (*Oreochromis niloticus*): effect of cortisol and homologous serum supplements from stressed and unstressed fish. *J. Membr. Biol.* **190**, 29-42.

Kirschner, L. B. (1970). The study of NaCl transport in aquatic animals. *Am. Zool.* **10**, 365-376.

Kobayashi, K. A. and Wood, C. M. (1980). The response of the kidney of the freshwater rainbow trout to true metabolic acidosis. *J. Exp. Biol.* **84**, 227-244.

Lauren, D. J. and McDonald, D. G. (1985). Effects of copper on branchial ionoregulation in the rainbow trout, *Salmo gairdneri* Richardson. *J. Comp. Physiol.* B **155**, 635-644.

Lewis, J. M., Costa, I., Val, A. L., Almeida-Val, V. M., Gamperl, A. K. and Driedzic, W. R. (2007). Responses to hypoxia and recovery: repayment of oxygen debt is not associated with compensatory protein synthesis in the Amazonian cichlid, *Astronotus ocellatus*. *J. Exp. Biol.* **210**, 1935-1943.

Loretz, C. A. (1979). Water exchange across fish gills: the significance of tritiated-water flux measurements. *J. Exp. Biol.* **79**, 147-162.

Lyndon, A. R. (1994). A method for measuring oxygen consumption in isolated perfused gills. *J. Fish. Biol.* **44**, 707-715.

Marshall, W. S. and Grosell, M. (2006). Ion transport and osmoregulation in fish. In *The Physiology of Fishes*, 3rd edn (ed. D. Evans), pp. 177-230. Boca Raton, FL: CRC Press.

Matey, V., Richards, J. G., Wang, Y., Wood, C. M., Rogers, J., Davies, R., Murray, B. W., Chen, X. Q., Du, J. and Brauner, C. J. (2008). The effect of hypoxia on gill morphology and ionoregulatory status in the Lake Qinghai scaleless carp, *Gymnocypris przewalskii*. *J. Exp. Biol.* **211**, 1063-1074.

McDonald, D. G. and Rogano, M. S. (1986). Ion regulation by the rainbow trout, *Salmo gairdneri*, in ion-poor water. *Physiol. Zool.* **59**, 318-331.
McDonald, D. G., Cavdek, V. and Ellis, R. (1991). Gill design in freshwater fishes: interrelationships among gas exchange, ion regulation, and acid-base regulation. *Physiol. Zool.* **64**, 103-123.
McDonald, M. D., Smith, C. P. and Walsh, P. J. (2006). The physiology and evolution of urea transport in fishes. *J. Membr. Biol.* **212**, 93-107.
McWilliams, P. G. and Potts, W. T. W. (1978). The effects of pH and calcium concentrations on gill potentials in the brown trout, *Salmo trutta*. *J. Comp. Physiol.* **126**, 277-286.
Morgan, J. D. and Iwama, G. K. (1999). Energy cost of NaCl transport in isolated gills of cutthroat trout. *Am. J. Physiol.* **277**, R631-R639.
Motais, R., Isaia, J., Rankin, J. C. and Maetz, J. (1969). Adaptive changes of the water permeability of the teleostean gill epithelium in relation to external salinity. *J. Exp. Biol.* **51**, 529-546.
Munger, R. S., Reid, S. D. and Wood, C. M. (1991). Extracellular fluid volume measurements in tissues of the rainbow trout (*Oncorhynchus mykiss) in vivo* and their effects on intracellular pH and ion calculations. *Fish Physiol. Biochem.* **9**, 313-322.
Muusze, B., Marcon, J., van den Thillart, G. and Almeida-Val, V. (1998). Hypoxia tolerance of Amazon fish; respirometry and energy metabolism of the cichlid *Astronotus ocellatus*. *Comp. Biochem. Physiol.* **A120**, 151-156.
Nakada, T., Westhoff, C. M., Kato, A. and Hirose, S. (2007). Ammonia secretion from fish gill depends on a set of Rh proteins. *FASEB J.* **21**, 1-8.
Nawata, C. M., Hung, C. C. Y., Tsui, T. K. N., Wilson, J. M., Wright, P. A. and Wood, C. M. (2007). Ammonia excretion in rainbow trout (*Oncorhynchus mykiss*): evidence for Rh glycoprotein and H^+-ATPase involvement. *Physiol. Genomics* **31**, 463-474.
Nilsson, G. E. (2007). Gill remodeling in fish: a new fashion or an ancient secret? *J. Exp. Biol.* **210**, 2403-2409.
Olson, K. R. (1992). Blood and extracellular fluid volume regulation. In *Fish Physiology*, vol. 12B (ed. W. S. Hoar, D. J. Randall and A. P. Farrell), pp. 135-254. San Diego, CA: Academic Press.
Patel, M., Iftikar, F. I., Smith, R. W., Ip, Y. K. and Wood, C. M. (2009). Water balance and renal function in two species of African lungfish *Protopterus dolloi* and *Protopterus annectens*. *Comp. Biochem. Physiol. A* **152**, 149-157.
Postlethwaite, E. and McDonald, D. G. (1995). Mechanisms of Na^+ and Cl^- regulation in freshwater-adapted rainbow trout (*Oncorhynchus mykiss*) during exercise and stress. *J. Exp. Biol.* **198**, 295-304.
Potts, W. T. W. (1984). Transepithelial potentials in fish gills. In *Fish Physiology*, vol. 10B (ed. W. S. Hoar and D. J. Randall), pp. 105-128. Orlando, FL: Academic Press.
Potts, W. T. W. and Eddy, F. B. (1973). Gill potentials and sodium fluxes in the flounder *Platichthys flesus*. *J. Comp. Physiol.* **87**, 20-48.
Potts, W. T., Foster, M. A., Rudy, P. P. and Howells, P. G. (1967). Sodium and water balance in the cichlid teleost, *Tilapia mossambica*. *J. Exp. Biol.* **47**, 461-470.
Randall, D. J., Holeton, G. F. and Stevens, E. D. (1967). The exchange of oxygen and carbon dioxide across the gills of rainbow trout. *J. Exp. Biol.* **46**, 339-348.
Randall, D. J., Baumgarten, D. and Malyusz, M. (1972). The relationship between gas and ion transfer across the gills of fishes. *Comp. Biochem. Physiol.* **41A**, 629-637.
Richards, J. G., Wang, Y. S., Brauner, C. J., Gonzalez, R. J., Patrick, M. L., Schulte, P. M., Choppari-Gomes, A. R., Almeida-Val, V. M. F. and Val, A. L. (2007). Metabolic and ionoregulatory responses of the Amazonian cichlid, *Astronotus ocellatus*, to severe hypoxia. *J. Comp. Physiol. B* **177**, 361-374.
Schwerte, T., Uberbacher, D. and Pelster, B. (2003). Non-invasive imaging of blood cell concentration and blood distribution in zebrafish *Danio rerio* incubated in hypoxic conditions *in vivo*. *J. Exp. Biol.* **206**, 1299-1307.
Scott, G. R., Rogers, J. T., Richards, J. G., Wood, C. M. and Schulte, P. M. (2004). Intraspecific divergence of ionoregulatory physiology in the euryhaline teleost *Fundulus heteroclitus*: possible mechanisms of freshwater adaptation. *J. Exp. Biol.* **207**, 3399-3410.
Scott, G. R., Wood, C. M., Sloman, K. A., Iftikar, F. I., De Boeck, G., Almeida-Val, V. M. and Val, A. L. (2008). Respiratory responses to progressive hypoxia in the Amazonian oscar, *Astronotus ocellatus*. *Respir. Physiol. Neurobiol.* **162**, 109-116.
Sioli, H. (1984). The Amazon and its main affluents: hydrography, morphology of the river courses, and river types. In *The Amazon: Limnology and Landscape Ecology of a Mighty Tropical River and its Basin* (ed. H. Sioli), pp. 127-166. Dordrecht: DRW Junk.
Sloman, K. A., Wood, C. M., Scott, G. R., Wood, S., Kajimura, M., Johannsson, O. E., Almeida-Val, V. M. F. and Val, A. L. (2006). Tribute to R. G. Boutilier: the effect of size on the physiological and behavioural responses of oscar, *Astronotus ocellatus*, to hypoxia. *J. Exp. Biol.* **209**, 1197-1205.
Sollid, J. and Nilsson, G. E. (2006). Plasticity of respiratory structures: adaptive remodelling of fish gills induced by ambient oxygen and temperature. *Respir. Physiol. Neurobiol.* **154**, 241-251.
Sollid, J., De Angelis, P., Gundersen, K. and Nilsson, G. E. (2003). Hypoxia induces adaptive and reversible gross morphological changes in crucian carp gills. *J. Exp. Biol.* **206**, 3667-3673.
Sollid, J., Weber, R. E. and Nilsson, G. E. (2005). Temperature alters the respiratory surface area of Crucian carp *Carassius carassius* and goldfish *Carassius auratus*. *J. Exp. Biol.* **208**, 1109-1116.
Swift, D. J. and Lloyd, R. (1974). Changes in urine flow rate and haematocrit value of rainbow trout *Salmo gairdnei*i (Richardson) exposed to hypoxia. *J. Fish. Biol.* **6**, 379-387.
Tervonen, V., Vuolteenaho, O. and Nikinmaa, M. (2006). Haemoconcentration *via* diuresis in short-term hypoxia: a possible role for cardiac natriuretic peptide in rainbow trout. *Comp. Biochem. Physiol.* **144A**, 86-92.
Val, A. L. and Almeida-Val, V. M. F. (1995). *Fishes of the Amazon and Their Environment*. Berlin: Springer.
van den Thillart, G. and Kesbeke, F. (1978). Anaerobic production of carbon dioxide and ammonia by goldfish, *Carassius auratus* L. *Comp. Biochem. Physiol.* **59A**, 393-400.
van Waarde, A. (1983). Aerobic and anaerobic ammonia production by fish. *Comp. Biochem. Physiol.* **74B**, 675-684.
Verdouw, H., van Echted, C. J. A. and Dekkers, E. M. J. (1978). Ammonia determination based on indophenol formation with sodium salicylate. *Water Res.* **12**, 399-402.
Wilkie, M. P. (2002). Ammonia excretion and urea handling by fish gills: present understanding and future research challenges. *J. Exp. Zool.* **293**, 284-301.
Wolf, K. (1963). Physiological salines for fresh-water teleosts. *Prog. Fish Cult.* **25**, 135-140.
Wood, C. M. (1988). Acid–base and ionic exchanges at gills and kidney after exhaustive exercise in the rainbow trout. *J. Exp. Biol.* **146**, 461-481.
Wood, C. M. (1992). Flux measurements as indices of H^+ and metal effects on freshwater fish. *Aquat. Toxicol.* **22**, 239-264.
Wood, C. M. and Grosell, M. (2008). A critical analysis of transepithelial potential in intact killifish (*Fundulus heteroclitus*) subjected to acute and chronic changes in salinity. *J. Comp. Physiol. B* **178**, 713-727.
Wood, C. M. and Laurent, P. (2003). Na^+ *versus* Cl^- transport in the intact killifish after rapid salinity transfers. *Biochim. Biophys. Acta* **1618**, 106-120.
Wood, C. M. and Pärt, P. (1997). Cultured branchial epithelia from freshwater fish gills. *J. Exp. Biol.* **200**, 1047-1059.
Wood, C. M. and Patrick, M. L. (1994). Methods for assessing kidney and urinary bladder function in fish. In *Biochemistry and Molecular Biology of Fishes*, vol. 3 (ed. P. W. Hochachka and T. P. Mommsen), pp. 127-143. New York: Elsevier.
Wood, C. M. and Randall, D. J. (1973a). The influence of swimming activity on sodium balance in the rainbow trout (*Salmo gairdneri*). *J. Comp. Physiol.* **82**, 207-233.
Wood, C. M. and Randall, D. J. (1973b). The influence of swimming activity on water balance in the rainbow trout (*Salmo gairdneri*). *J. Comp. Physiol.* **82**, 257-276.
Wood, C. M., McMahon, B. R. and McDonald, D. G. (1978). Oxygen exchange and vascular resistance in the totally perfused rainbow trout. *Am. J. Physiol.* **234**, R201-R208.
Wood, C. M., Wilson, R. W., Gonzalez, R. J., Patrick, M. L., Bergman, H. L., Narahara, A. and Val, A. L. (1998). Responses of an Amazonian teleost, the tambaqui (*Colossoma macropomum*) to low pH in extremely soft water. *Physiol. Biochem. Zool.* **71**, 658-670.
Wood, C. M., Kajimura, M., Sloman, K. A., Scott, G. R., Walsh, P. J., Almeida-Val, V. M. F. and Val, A. L. (2007). Rapid regulation of Na^+ fluxes and ammonia excretion in response to acute environmental hypoxia in the Amazonian oscar, *Astronotus ocellatus*. *Am. J. Physiol.* **292**, R2048-R2058.